CHAPTER 8: RADIOGENIC ISOTOPE GEOCHEMISTRY

8.1 INTRODUCTION

R adiogenic isotope geochemistry had an enormous influence on geologic thinking in the twentieth century. The story begins, however, in the late nineteenth century. At that time Lord Kelvin (born William Thomson, and who profoundly influenced the development of physics and thermodynamics in the 19th century), estimated the age of the solar system to be about 100 million years, based on the assumption that the Sun's energy was derived from gravitational collapse. In 1897 he revised this estimate downward to the range of 20 to 40 million years. A year earlier, another Englishman, John Jolly, estimated the age of the Earth to be about 100 million years based on the assumption that salts in the ocean had built up through geologic time at a rate proportional their delivery by rivers. Geologists were particularly skeptical of Kelvin's revised estimate, feeling the Earth must be older than this, but had no quantitative means of supporting their arguments. They did not realize it, but the key to the ultimate solution of the dilemma, radioactivity, had been discovered about the same time (1896) by Frenchman Henri Becquerel. Only eleven years elapsed before Bertram Boltwood, an American chemist, published the first 'radiometric age'. He determined the lead concentrations in three samples of pitchblende, a uranium ore, and concluded they ranged in age from 410 to 535 million years. In the meantime, Jolly also had been busy exploring the uses of radioactivity in geology and published what we might call the first book on isotope geochemistry in 1908. When the dust settled, the evidence favoring an older Earth was deemed conclusive.

Satisfied though they might have been with this victory, geologists remained skeptical of radiometric age determinations. One exception was Arthur Holmes, who in 1913 estimated that the oldest rocks were at least 1600 million years old (Holmes was exceptional as well in his support for Alfred Wegener's hypothesis of continental drift). Many geologists were as unhappy with Holmes's age for the Earth as they had been with Kelvin's.

Until the end of World War II, the measurement of isotope ratios was the exclusive province of physicists. One name, that of Alfred Nier, stands out over this period. Nier determined the isotopic compositions of many elements and made the first measurements of geologic time based on isotope ratios rather than elemental abundances. Modern mass spectrometers, while vastly more sophisticated than those of a half century ago, have evolved from Nier's 1940 design. After World War II, mass spectrometers began to appear in geological laboratories. Many of these laboratories were established by former students and associates of Nier or Harold Urey of the University of Chicago. As this occurred, isotope geochemistry expanded well beyond geochronology, ultimately to have an impact in almost every branch of earth science.

Beyond providing precise ages of geologic events, radioactive decay is important because it provides natural tracers of geologic processes and because it provides information on the rates and pathways of geologic evolution. To understand the first point, consider a biologist who wishes to know how a nutrient, phosphorus for example, is utilized by an organism, a horse for example. The biologist can feed the horse grain doped with a small amount of radioactive phosphorus. Then by taking tissue and fluid samples and determining the amount of radioactive phosphorous present, he can trace phosphorus through various metabolic pathways. Similarly, an engineer might test a new automobile design by placing a model in a wind tunnel and using smoke as a tracer to follow the path of air around it. In principle at least, we could do a similar thing with the Earth. We might add dye to downwelling ocean water to trace deep ocean currents, or add a radioactive tracer to subducting lithosphere to trace mantle convection currents. In practice, however, even the contemplation of such experiments is a bit absurd. We would need far too much dye or radioactive tracer: the scales of distance and mass are simply too large for this kind of experiment. Even if we could overcome that obstacle, we would be long dead before any useful results came from our experiment: the rates of geologic processes are simply too slow.

Nature, however, has provided natural tracers in the form of the radiogenic isotopes, which are products of natural radioactivity, and these tracers have been moving through the Earth since its beginning. For example, subducting oceanic crust has a different ratio of ^{87}Sr to ^{86}Sr than does the mantle,

so we can use the $^{87}Sr/^{86}Sr$ ratio to trace the flow of subducting lithosphere through the mantle. Similarly, Atlantic water has a lower $^{143}Nd/^{144}Nd$ ratio than does Pacific water, so we can trace the flow of North Atlantic Deep Water into the Pacific using the $^{143}Nd/^{144}Nd$ ratio.

To understand the second point, consider the continental crust, which has a much higher ratio of Rb to Sr than does the mantle. Through time, this has led to a higher ratio of ^{87}Sr, the product of radioactive decay of ^{87}Rb, to ^{86}Sr in the crust than the mantle. However, the $^{87}Sr/^{86}Sr$ ratio in crustal rocks is lower than it should be had these rocks had their present Rb/Sr ratio for 4500 million years. From this observation we can conclude that the crust has not existed, or at least has not had its present composition, for the full 4500 million year history of the Earth. The situation is just the opposite for the mantle: had it had its present Rb/Sr ratio for 4500 million years it should have a lower $^{87}Sr/^{86}Sr$ than it does. Apparently, the mantle has had a higher Rb/Sr ratio in the past. From these simple observations we can draw the inference that the crust has evolved from the mantle through time. With more quantitative observations we can use isotope ratios to estimate the *rate* of crustal evolution.

Two fundamental assumptions are involved in virtually all geologic uses of radiogenic isotope ratios. The first is that the rate of radioactive decay is independent of all external influences, such as temperature, pressure, etc.   The second is that two isotopes of the same element are chemical identical and therefore that chemical processes cannot change, or fractionate, the ratio of two isotopes of the same elements. Neither of these assumptions holds in the absolute*. Nevertheless, all available evidence indicates violations of these assumptions are entirely negligible.

8.2 Physics of the Nucleus and the Structure of Nuclei

Nuclear physics is relevant to geochemistry for two reasons. First, the study of the distribution of isotopes forms an increasingly important part of geochemistry as well as earth science generally. Second, geochemistry concerns itself not only with the distribution of elements, but also with their origin, and the elements originated through nuclear processes.

Nuclei are made up of various numbers of neutrons and protons. We'll use N to represent the number of neutrons, the *neutron number*, and Z to represent the number of protons, or *proton number*. Z is also the *atomic number* of the element, because the chemical properties of elements depend almost exclusively on the number of protons (since in the neutral atom the number of electrons equals the number of protons). The sum of Z and N is the mass number A.

8.2.1 Nuclear Structure and Energetics

Not all possible combinations of protons and neutrons result in stable nuclei. Typically for stable nuclei, N ≈ Z. Thus a significant portion of the nucleus consists of protons, which tend to repel each other. From the observation that nuclei exist at all, it is apparent that another force must exist which is stronger than coulomb repulsion at short distances. It must be negligible at larger distances, otherwise all matter would collapse into a single nucleus. This force, called the nuclear force, is a manifestation of one of the fundamental forces of nature (or a manifestation of the single force in nature if you prefer unifying theories), called the *strong* force. If this force is assigned a strength of 1, then the strengths of other forces are: electromagnetic 10^{-2}; weak force 10^{-5}; gravity 10^{-39} (we will discuss the weak nuclear force shortly). Just as electromagnetic forces are mediated by a particle, the photon, the nuclear force is mediated by the pion. The photon carries one quantum of electromagnetic force field; the pion carries one quantum of nuclear force field. The strong force also binds quarks together to form hadrons, a class of particles that includes neutrons and protons. The intensity of the strong force decreases rapidly with distance, so that at distances more than about 10^{-14} m it is weaker than the electromagnetic force.

---

* There is a slight dependence of the rate of electron capture on pressure, and at extreme temperatures where nuclei become thermally excited there could be a dependence of decay rate on temperature (such temperatures, however, will only occur in the interiors of stars). There are subtle differences in the chemical behavior of the different isotopes of an element, which can be exploited for geological use, as we shall see in the next Chapter. For most radiogenic elements, 'isotopic fractionations' are small and corrections for them are easily and routinely made.

One of the rules of thermodynamics was that the configuration with the lowest Gibbs Free Energy is the most stable. This is really just one example of the general physical principle that the lowest energy configuration is the most stable; this rule applies to electron orbital configurations, as we saw in crystal field theory, and to nuclei. We would thus expect that if ^{4}He is stable relative to two free neutrons and two free protons, ^{4}He must be a lower energy state compared to the free particles. If this is the case, then from Einstein's mass-energy equivalence:

$$E = mc^2 \qquad 8.1$$

we can predict that the ^{4}He nucleus will have less mass that 2 free neutrons and protons. It does in fact have less

Figure 8.1 Binding energy per nucleon vs. mass number.

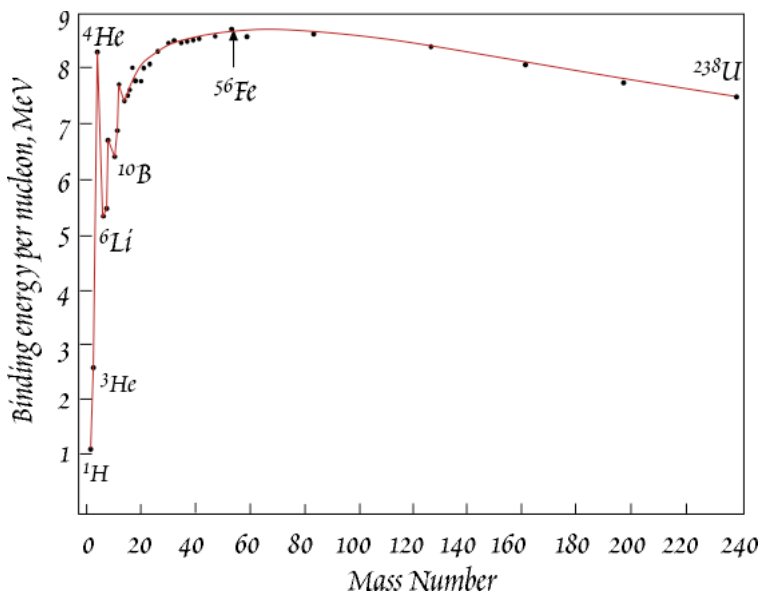mass. From the principle that the lowest energy configurations are the most stable and the mass-energy equivalen

We begin by calculating the nominal weight of an atom from the sum of the mass of the constituent particles:

proton: 1.007593 unified atomic mass unit (u) or Dalton (Da)[*] = 1.6726231 x 10^{-27} kg
neutron: 1.008982 u
electron: 0.000548756 u = 9.10093897 x 10^{-31} kg

Then we define the *mass decrement* of an atom as:

$$\delta = W - M \qquad\qquad 8.2$$

where W is the sum of the mass of the constituent particles and M is the actual mass of the atom. For example, W for ^{4}He is W = $2m_p + 2m_n + 2m_e$ = 4.034248 u. The mass of ^{4}He is 4.003873 u, so δ = 0.030375 u. Converting this to energy using Equ. 1 yields 28.28 Mev. This energy is known as the *binding energy*. Dividing by A, the mass number, or number of nucleons, gives the *binding energy per nucleon*, E_b:

$$E_b = \frac{W - M}{A} c^2 \qquad\qquad 8.3$$

E_b is a measure of nuclear stability: those nuclei with the largest binding energy per nucleon are the most stable. Figure 8.1 shows E_b as a function of mass. Note that the nucleons of intermediate mass tend to be the most stable.

Some indication of the relative strength of the nuclear binding force can be obtained by comparing the mass decrement associated with it to that associated with binding an electron to a proton in a hydrogen atom. The mass decrement above is of the order of 1%, 1 part in 10^2. The mass decrement associated with binding an electron to a nucleus of the order of 1 part in 10^8, so bonds between nucleons are about 10^6 times stronger than bonds between electrons and nuclei.

Why are some combinations of N and Z more stable than others? The answer has to do with the forces between nucleons and to how nucleons are organized within the nucleus. The structure and organization of the nucleus are questions still being actively researched in physics, and full treatment is certainly beyond the scope of this book, but we can gain some valuable insight to nuclear stability by considering two of the simplest models of nuclear structure. The simplest model of the nucleus is the *liquid-drop model*, proposed by Niels Bohr in 1936. This model assumes all nucleons in a nucleus have equivalent states. As its name suggests, the model treats the binding between nucleons as similar to the

---

[*] The was formerly called an *atomic mass unit* or *amu*. The unified atomic mass unit or Dalton is defined as 1/12th the mass of a ^{12}C atom. 1 u = 1.6605402 x 10^{-27} kg. Both u and *Da* are equivalent and acceptable SI units. The *unified atomic mass unit* seems preferred in physics and related fields while the *Dalton* seems preferred in biochemistry.

EXAMPLE 8.1. CALCULATING BINDING ENERGIES

Calculate the binding energies of ^{50}V, ^{50}Cr, and ^{50}Ti. Which of these 3 nuclei is the least stable? Which is the most stable?

Answer: the nucleus of ^{50}V consists of 23 protons and 27 neutrons, that of ^{50}Cr consists of 24 protons and 26 neutrons, that of ^{50}Ti consists of 22 protons and 28 neutrons. Atoms of these elements also have, respectively 23, 24, and 22 electrons. First we calculate W for each:

W $(^{50}$V$) = 23 \times 1.007593 + 27 \times 1.008982 + 23 \times 0.000548756 = 50.429774$ u

W $(^{50}$Cr$) = 24 \times 1.007593 + 26 \times 1.008982 + 24 \times 0.000548756 = 50.428934$ u

W $(^{50}$Ti$) = 22 \times 1.007593 + 28 \times 1.008982 + 22 \times 0.000548756 = 50.430615$ u

The actual masses (M) of these nuclides are: ^{50}V: 49.947162 u; ^{50}Cr: 49.946047 u; ^{50}Ti: 49.944792 u. Using equation 8.2 we calculate the mass decrement, and then divide by 50 to calculate the mass decrement per nucleon. We convert the result to kg using the conversion factor 1 dalton = 1.66×10^{-27} kg. We then multiply by the square of the speed of light (2.998×10^{8} m/sec) to obtain the binding energy in kg-m/sec or joules. We use 1 J = 6.2415×10^{12} MeV to convert our answer to MeV. The results are shown in the table below.

Nuclide	δ	δ	δ/A	E_b	E_b
	u	kg	kg/nucleon	J/nucleon	MeV
^{50}V	0.482612	8.011449×10^{-28}	1.60229×10^{-29}	1.4401×10^{-12}	8.9885
^{50}Cr	0.482887	8.016014×10^{-28}	1.60320×10^{-29}	1.4410×10^{-12}	8.9937
^{50}Ti	0.484568	8.043919×10^{-28}	1.60878×10^{-29}	1.4460×10^{-12}	9.0245

Our results indicate that of the three, ^{50}V is the least stable and ^{50}Ti the most stable, though the difference is not that great.
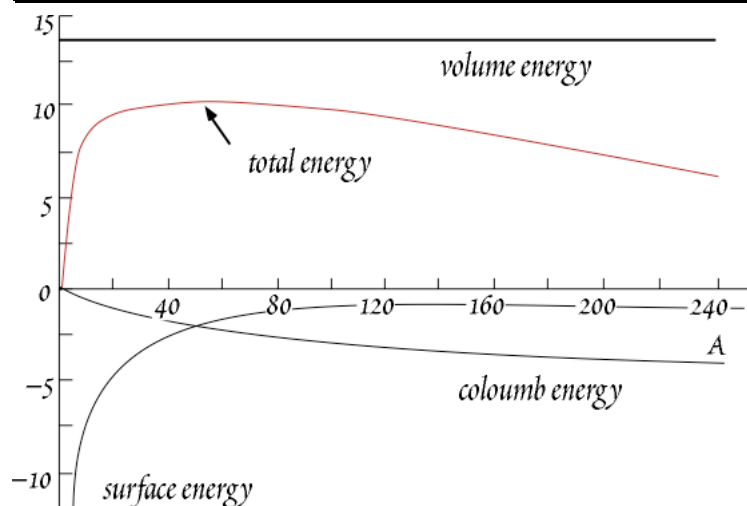

Figure 8.2. Binding energy per nucleon vs. mass number.

binding between molecules in a liquid drop. According to the liquid-drop model, the total binding of nucleons is influenced by 3 effects: a volume energy, a surface energy, and a coulomb energy. The variation of these three forces with mass number and their total effect is shown in Figure 8.2.

Looking again at Figure 8.1, we see that, except for very light nuclei, the binding energy per nucleon is roughly constant, or that total binding energy is roughly proportional to the number of nucleons. Similarly, for a drop of liquid, the energy required to evaporate it, or unbind the molecules, would be proportional to the volume of the liquid. So the volume effect contributes a constant amount of energy per nucleon.

The surface effect arises from saturation of the strong nuclear force: a nucleon in the interior of the nucleus is surrounded by other nucleons and exerts no force on more distance nucleons. But at the surface, the force is unsaturated, leading to a force similar to surface tension in liquids. This force tends to minimize the surface area of the nucleus. The surface force is strongest for light nuclei and becomes rapidly less important for heavier nuclei.

The third effect on nuclear stability considered by the liquid drop model is the repulsive force between protons. This force is a longer range one than the strong force and does not show saturation. It is proportional to the total number of proton pairs ($Z(Z – 1)/2$) and inversely proportional to radius. Figure 8.3 shows the stable combinations of N and Z on a plot of N against Z. Clearly, for light iso-

topes, N must roughly equal Z for a nucleus to be stable. For heavier isotopes the field of stability moves in the direction of N > Z. This effect may also be explained by the repulsive Coulomb force of the protons. The additional neutrons act to dilute the charge density (increase the radius) and thereby increase stability.

The liquid drop model can account for the general pattern of binding energy in Figure 8.1 and the general distribution of stable nuclei in Figure 8.3, but not the details. The model predicts a smooth variation in binding energy with mass number, but it is apparent from Figure 8.1 that this is not the case: certain maxima occur and some configurations are more stable than others. From this, we might guess that the nucleus has some internal structure.

Another interesting observation is the distribution of stable nuclei. Nuclei with even number of protons and neutrons are more stable than those with odd numbers of protons or neutrons. As Table 8.1 shows, stable even-even configurations are most common; stable odd-odd configurations are particularly rare. In addition, as can be seen in Figure 8.3, stable nuclei seem to be particularly common at *magic numbers*, i.e., when either N or Z equals 2, 8, 20, 28, 50, 82, and 126. These observations, the even number effect and the magic number effect, lead to the *shell model of the nucleus*. It is similar to the shell model of electron structure and is based on the same physical principles, namely the Pauli exclusion principle and quantum mechanics. The Pauli exclusion principle says that no state occupied by one nucleon can be occupied by another nucleon; i.e., a nucleon added to a nucleus must occupy a new state, or niche.

These states can be described by quantum numbers. One of these quantum numbers is spin. Two protons can have the same spatial quantum numbers if their spins are anti-aligned (the situation is analogous to electrons sharing orbits). This is also true of neutrons. Apparently, nuclei are more stable when spins cancel (i.e., even number of protons or neutrons). The first proton and neutron shells are filled when occupied by 2 nucleons each. As in the atomic model, filling these shells produces a particularly stable configuration. The next shells are filled when 6 additional protons and neutrons are added for a total of 8 (each). This configuration is ^{16}O. And so on, shells being filled with 2, 8, 20, 28, 50, 82, and 126 nucleons. These numbers of nucleons, which correspond to particularly stable nuclei, were called 'magic numbers' and were an important clue leading to the shell model.

Another important aspect of the shell model is its prediction of nuclear angular momentum. Even-even nuclei have no angular momentum because the spins of the neutrons cancel by anti-alignment, as do the proton spins. And the angular orbital momentum is zero because the nucleons are in closed shells. In even-odd and odd-even nuclides one odd nucleon combines its half integral spin with the integral orbital angular momentum quantum number of the nucleus yielding half-integral angular momentum. In odd-odd nuclei, the odd proton and odd neutron each contribute a
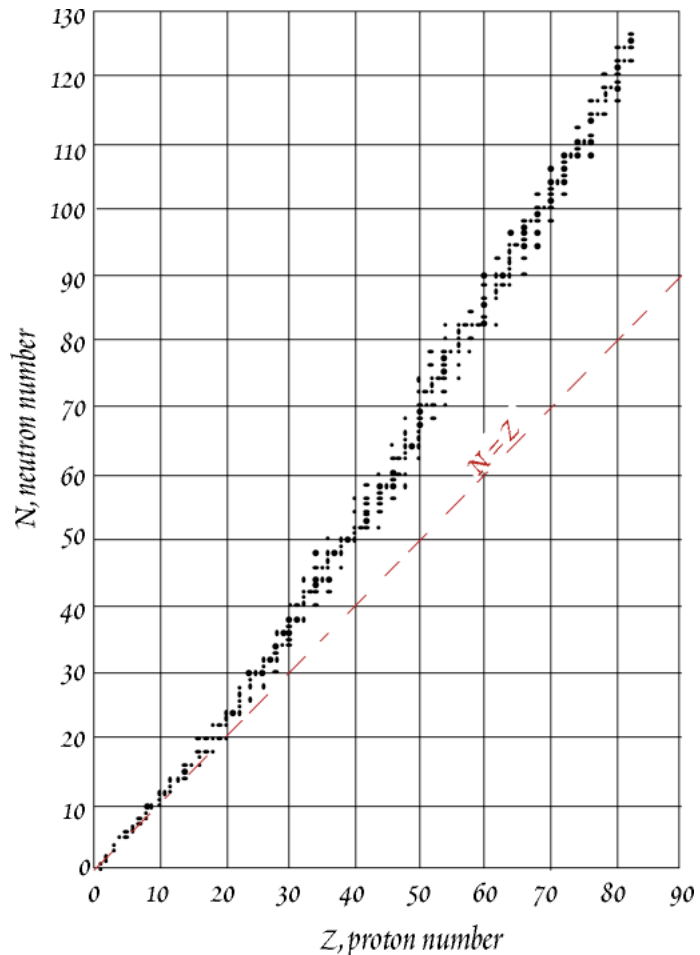

Figure 8.3. Neutron number vs. proton number for stable nuclides.

Table 8.1. Numbers of Stable Odd and Even Nuclei

Z	N	A (Z + N)	number of stable nuclei	number of very long-lived nuclei
odd	odd	even	4	5
odd	even	odd	50	3
even	odd	odd	55	3
even	even	even	165	11

spin of 1/2 yielding an integral angular momentum, which can combine with an integral orbital angular momentum quantum number to produce an integral angular momentum.

A slightly more complex model is called the *collective model*. It is intermediate between the liquid-drop and the shell models. It emphasizes the collective motion of nuclear matter, particularly the vibrations and rotations, both quantized in energy, in which large groups of nucleons can participate. Even-even nuclides with Z or N close to magic numbers are particularly stable with nearly perfect spherical symmetry. Spherical nuclides cannot rotate because of a dictum of quantum mechanics that a rotation about an axis of symmetry is undetectable, and hence cannot exist, and in a sphere every axis is a symmetry axis. The excitation of such nuclei (that is, when their energy rises to some quantum level above the ground state) may be ascribed to the vibration of the nucleus as a whole. On the other hand, even-even nuclides far from magic numbers depart substantially from spherical symmetry and the excitation energies of their excited states may be ascribed to rotation of the nucleus.

8.2.2 The Decay of Excited and Unstable Nuclei

Just as an atom can exist in any one of a number of excited states, so too can a nucleus have a set of discrete, quantized, excited nuclear states. The behavior of nuclei in transforming to more stable states is somewhat similar to atomic transformation from excited to more stable sites, but there are some important differences. First, energy level spacing is much greater; second, the time an unstable nucleus spends in an excited state can range from 10^{-14} sec to 10^{11} years, whereas atomic life times are usually about 10^{-8} sec; third, excited atoms emit photons, but excited nuclei may emit other particles as well as photons. The photon emitted through the decay of unstable nuclei is called a gamma ray. Nuclear reactions must obey general physical laws, conservation of momentum, mass-energy, spin, etc. and conservation of nuclear particles. In addition to the decay of an excited nucleus to a more stable state, it is also possible for an unstable nucleus to decay to an entirely different nucleus, through the emission or absorption of a particle of non-zero rest mass.

Nuclear decay takes place at a rate that follows the law of radioactive decay. Interestingly, the decay rate is dependent only on the nature and energy state of the nuclide. It is independent of the past history of the nucleus, and essentially independent of external influences such as temperature, pressure, etc. Also, it is impossible to predict when a given nucleus will decay. We can, however, predict the probability of its decay in a given time interval. The probability of decay of a nucleus in some time interval, dt, is λ, where λ is called the decay constant. The probability of a decay among some number, N, of nuclides within dt is λN. Therefore, the rate of decay of N nuclides is:

$$\boxed{\frac{dN}{dt} = -\lambda N}$$ 8.4

The minus sign simply indicates N decreases with time. Equation 8.4 is a first-order rate law that we will call the *Basic Equation of Radioactive Decay*. It is very much analogous to rate equations for chemical reactions (Chapter 5), and in this sense λ is exactly analogous to k, the rate constant, for chemical reactions, except that λ is independent of all other factors.

8.2.2.1 GAMMA DECAY

Gamma emission occurs when an excited nucleus decays to a more stable state. A gamma ray is simply a high-energy photon (i.e., electromagnetic radiation). Its frequency, ν, is related to the energy difference by:

$$hv = E_u - E_l \qquad\qquad 8.5$$

where E_u and E_l are the energies of the upper (excited) and lower (ground) states and h is Planck's constant. The nuclear reaction is written as:

$$^{N}Z^* \rightarrow {}^{N}Z + \gamma \qquad\qquad 8.6$$

where Z is the element symbol, N is the mass number, and γ denotes the gamma ray.

8.2.2.2 ALPHA DECAY

An α-particle is simply a helium nucleus. Since the helium nucleus is particularly stable, it is not surprising that such a group of particles might exist within the parent nucleus before α-decay. Emission of an alpha particle decreases the mass of the nucleus by the mass of the alpha particle plus a mass equivalent to the energy lost during the decay, which includes the kinetic energy of the alpha particle (constant for any given decay) and the remaining nucleus (because of the conservation of momentum, the remaining nucleus recoils from the decay reaction), and any gamma ray emitted.

The escape of the α particle is a bit of a problem, because it must overcome a very substantial energy barrier, a combination of the strong force and the coulomb repulsion, to get out. For example, α particles with energies below 8 Mev are scattered from the ^{238}U nucleus. However, the α particle emerges from the decaying ^{238}U with an energy of only about 4 Mev. This is an example of a quantum mechanical effect called *tunneling* and can be understood as follows. Quantum mechanics holds that we can never know exactly where the α particle is (or any other particle, or you or I for that matter), we only the know the probability of its being in a particular place. This probability is determined by the square of the particle's wave function, ψ. Although the wave is strongly attenuated through the potential energy barrier, it nevertheless has a small but finite amplitude outside the nucleus, and hence there is a small but finite probability of the α particle being located outside the nucleus. Anything that can occur ultimately will, so sooner or later the alpha particle escapes the nucleus.

The daughter may originally be in an excited state, from which it decays by γ decay. Figure 8.4 shows an energy-level diagram for such a decay.

Alpha-decay occurs in nuclei with masses above the maximum in the binding energy curve of Figure 8.1, located at ^{56}Fe. Quite possibly, all such nuclei are unstable relative to alpha-decay, but the half-lives of most of them are immeasurably long.
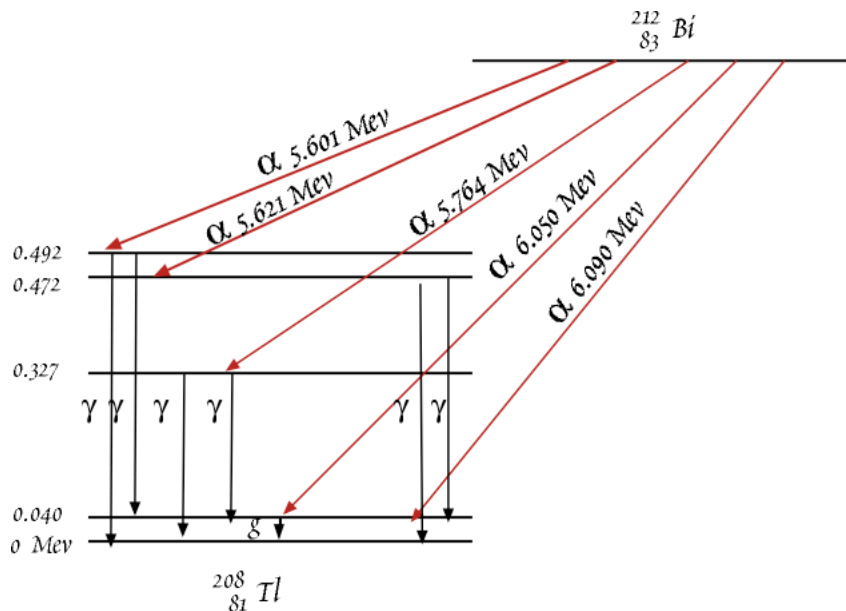

Figure 8.4. Nuclear energy-level diagram showing decay of bismuth 212 by alpha emission to the ground and excited states of thallium 208.

8.2.2.3 BETA DECAY

Beta decay is a process in which the charge of a nucleus changes, but not the number of nucleons. If we plotted Figure 8.3 with a third dimension, namely energy of the nucleus, we would see that stable nuclei are located in an energy valley. Alpha-decay moves a nucleus down the valley axis; beta decay moves a nucleus down the walls toward the valley axis. Beta-decay results in the emission of an electron or positron (a positively charged electron), depending on which side of the valley the parent lies. Consider the 3 nuclei in Figure 8.5. These are known as *isobars*, since they have the same number of nucleons(12; *isotopes* have the

same number of protons, *isotones* have the same number of neutrons). From what we know of nuclear structure, we can predict that the ^{12}C nucleus is the most stable of these three, because the spins of the neutrons and protons cancel each other. This is the case: ^{12}B decays to ^{12}C by the creation and emission of a β^- particle and the conversion of a neutron to a proton. ^{12}N decays by emission of a β^+ and conversion of a proton to a neutron.
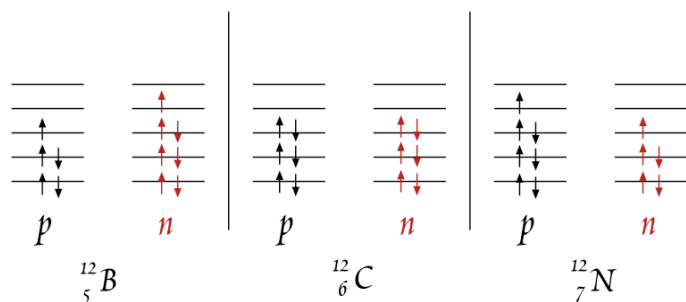

Figure 8.5. Proton and neutron occupation levels of boron 12, carbon 12 and nitrogen 12.

The discovery of beta decay presented physicists with a problem. Angular momentum must be conserved in the decay of nuclei. The ^{12}C nucleus has integral spin, as do ^{12}B and ^{12}N. But the beta particle (an electron or positron) has 1/2 quantum spin units, hence β decay apparently resulted in the loss of 1/2 spin units. The solution, proposed by Enrico Fermi[†], was another, essentially massless, particle called the *neutrino*, with 1/2 spin to conserve angular momentum. (Whether the neutrino has mass remains unresolved. The most recent observations and experiments have shown that the mass of the neutrino must be extremely small, and it is most likely massless.) It is also needed to balance energy. The kinetic energies of alpha particles are discrete. Not so for betas: they show a spectrum with a characteristic maximum energy for a given decay. Since energy must be conserved, and the total energy given off in any decay must be the same, it is apparent that the neutrino must also carry away part of the energy. The exact distribution of energy between the beta and the neutrino is random: it cannot be predicted in an isolated case, though there tends to be a fixed statistically distribution of energies, with the average observed beta energies being about 1/3 the maximum value (the maximum value is the case where the beta carries all the energy).

Beta decay involves the weak nuclear force. The weak force transforms a neutral particle into a charged one and visa versa. Both the weak and the electromagnetic force are now thought to be simply a manifestation of one force that accounts for all interactions involving charge (in the same sense that electric and magnetic forces are manifestations of electromagnetism). This force is called electroweak. In β^+ decay, for example, a proton is converted to a neutron, giving up its +1 charge to a neutrino, which is converted to a positron. This process occurs through the intermediacy of the W+ particle in the same way that electromagnetic processes are mediated by photons. The photon and W particles are members of a class of particles called *bosons* that mediate forces between the basic constituents of matter. However, W particles differ from photons in having a substantial mass.

8.2.2.4 ELECTRON CAPTURE

Another type of reaction is electron capture. This is sort of the reverse of beta decay and has the same effect, more or less, as β^+ decay. Interestingly, this is a process in which an electron is added to a nucleus to produce a nucleus with less mass than the parent! The missing mass is carried off as energy by an escaping neutrino, and in some cases by a γ. In some cases, a nucleus can decay by either electron capture, β^-, or β^+ emission. An example is the decay of ^{40}K, which decays to ^{40}Ar by β^+ or electron capture and to ^{40}Ca by β^-. In Example 8.1, we found that ^{50}V was less stable than it's 2 isobars: ^{50}Cr and ^{50}Ti. In fact, a ^{50}V atom will eventually decay to either a ^{50}Cr atom by β^- decay or to ^{50}Ti by electron capture. The half-life for this decay is 1.4×10^{17} years, so that the decay of any single atom of ^{50}V is extremely improbable.

β decay and electron capture often leave the daughter nucleus in an excited state. In this case, it will decay to its ground state (usually very quickly) by the emission of a γ-ray. Thus γ rays often ac-

---

[†]Enrico Fermi (1901-1954) had the unusual distinction of being both an outstanding theorist and an outstanding experimentalist. He made many contributions to quantum and nuclear physics and won the Nobel Prize in 1938. Interestingly, the journal *Nature* rejected the paper in which Fermi made this proposal!

company β decay. A change in charge of the nucleus necessitates a rearrangement of the electrons in their orbits. This rearrangement results in x-rays being emitted from electrons in the inner orbits.

8.2.2.5 SPONTANEOUS FISSION

Fission is a process in which a nucleus splits into two or more fairly heavy daughter nuclei. In nature, this is a very rare process, occurring only in the heaviest nuclei, ^{238}U, ^{235}U, and ^{232}Th (it is, however, most likely in ^{238}U). This particular phenomenon is perhaps better explained by the liquid drop model than the shell model. In the liquid drop model, the surface tension tends to minimize the surface area while the repulsive coulomb energy tends to increase it. We can visualize these heavy nuclei as oscillating between various shapes. The nucleus may very rarely become so distorted by the repulsive force of 90 or so protons, that the surface tension cannot restore the shape. Surface tension is instead minimized by the splitting the nucleus entirely. Since there is a tendency for the N/Z ratio to increase with A for stable nuclei, the parent is neutron-rich. When fission occurs, some free neutrons are produced and nuclear fragments (the daughters, which may range from A=30, zinc, to A=64, terbium) are too rich in neutrons to be stable. The immediate daughters will decay by β⁻ decay until enough neutrons have been converted to protons that it has reached the valley of energy stability. It is this tendency to produce unstable nuclear by-products, rather than fission itself, which makes fission in bombs and nuclear reactors such radiation hazards.

Some unstable heavy nuclei and excited heavy nuclei are particularly subject to fission. An important example is ^{236}U. Imagine a material rich in U. When one ^{238}U undergoes fission, some of the released neutrons are captured by ^{235}U nuclei, producing ^{236}U in an excited state. This ^{236}U then fissions producing more neutrons, etc. – a sustained chain reaction. This is the basis of nuclear reactors and bombs (actually, the latter more often use some other nuclei, like Pu). The concentration of U, and ^{235}U in particular, is not high enough for this sort of thing to happen naturally – fisson chain reactions require U enriched in ^{235}U. However, the concentration of ^{235}U was higher in the ancient Earth and at least one sustained natural chain reaction is known to have occurred about 2 billion years ago in the Oklo uranium deposit in Gabon, Africa. This deposit was found to have an anomalously low ^{235}U/^{238}U ratio, indicating some of the ^{235}U had been 'burned' in a nuclear chain reaction. Anomalously high concentrations of fission-produced nuclides confirmed that this had indeed occurred.

Individual fission reactions are less rare. When fission occurs, there is a fair amount of kinetic energy produced, the fragments literally flying apart. These fragments damage the crystal structure through which they pass, producing 'tracks', whose visibility can be enhanced by etching. This is the basis of *fission track dating*.

Natural fission also can produce variations in the isotopic abundance of the daughter elements. In general, however, the amount of the daughter produced is so small relative to that already present in the Earth, that these isotopic variations are immeasurably small. An important exception is xenon, whose isotopic composition can vary slightly due to contributions from fission of U and the extinct radionuclide ^{244}Pu.

8.3 BASICS OF RADIOGENIC ISOTOPE GEOCHEMISTRY

The basic equation of radioactive decay is:

$$\frac{dN}{dt} = -\lambda N \qquad (8.4)$$

λ is the decay constant, which we defined as the probability that a given atom would decay in some time dt. It has units of time^{-1}. Let's rearrange equation 8.4 and integrate:

$$\int_{N_0}^{N} \frac{dN}{N} = \int_{0}^{t} -\lambda t \qquad 8.7$$

where N_0 is the number of atoms of the radioactive, or parent, isotope present at time t=0. Integrating, we obtain:

$$\ln \frac{N}{N_0} = -\lambda t \qquad 8.8$$

This can be expressed as:
$$\frac{N}{N_0} = e^{-\lambda t} \qquad \text{or} \qquad N = N_0 e^{-\lambda t} \qquad \text{8.9}$$

Suppose we want to know the amount of time for the number of parent atoms to decrease to half the original number, i.e., t when $N/N_0 = 1/2$. Setting N/N_0 to $1/2$, we can rearrange 8.8 to get:

$$\ln \frac{1}{2} = -\lambda t_{1/2} \qquad \text{or} \quad \ln 2 = \lambda t_{1/2}$$

and finally:
$$t_{1/2} = \frac{\ln 2}{\lambda} \qquad \text{8.10}$$

This is the definition of the *half-life, $t_{1/2}$*.

Now the decay of the parent produces some daughter, or *radiogenic*, nuclides. The number of daughters produced is simply the difference between the initial number of parents and the number remaining after time t:

$$D = N_0 - N \qquad \text{8.11}$$

Rearranging 8.9 to isolate N_0 and substituting that into 8.11, we obtain:

$$D = N e^{\lambda t} - N = N(e^{\lambda t} - 1) \qquad \text{8.12}$$

This tells us that the number of daughters produced is a function of the number of parents present and time. Since in general there will be some atoms of the daughter nuclide around to begin with, i.e., when $t = 0$, a more general expression is:

$$\boxed{D = D_0 + N(e^{\lambda t} - 1)} \qquad \text{8.13}$$

where D_0 is the number of daughters originally present.

An exponential function can be expressed as a Taylor Series expansion:

$$e^{\lambda t} = 1 + \lambda t + \frac{(\lambda t)^2}{2!} + \frac{(\lambda t)^3}{3!} + \dots \qquad \text{8.14}$$

Provided $\lambda t \ll 1$, the higher order terms become very small and can be ignored; hence for times that are short compared to the decay constant (i.e., for $t \ll 1/\lambda$), equation 8.13 can be written as:

$$D \cong D_0 + N \lambda t \qquad \text{8.15}$$

Let's now write equation 8.13 using a concrete example, such as the decay of ^{87}Rb to ^{87}Sr:

$$^{87}\text{Sr} = {}^{87}\text{Sr}_0 + {}^{87}\text{Rb}(e^{\lambda t} - 1) \qquad \text{8.16}$$

As it turns out, it is generally much easier, and usually more meaningful, to measure to ratio of two isotopes than the absolute abundance of one. We therefore measure the ratio of ^{87}Sr to a non-radiogenic isotope, which by convention is ^{86}Sr. Thus the useful form of 8.16 is:

$$\frac{^{87}Sr}{^{86}Sr} = \left(\frac{^{87}Sr}{^{86}Sr} \right)_0 + \frac{^{87}Rb}{^{86}Sr} \left(e^{\lambda t} - 1 \right) \qquad \text{8.17}$$

Similar expressions can be written for other decay systems.

Equation 8.17 is a concise statement of Sr isotope geochemistry: the ^{87}Sr/^{86}Sr ratio in a system depends on: (1) the ^{87}Sr/^{86}Sr at time t = 0, (2) the ^{87}Rb/^{86}Sr ratio of the system (in most cases, we can assume the ^{87}Rb/^{86}Sr ratio is directly proportional to the Rb/Sr ratio), and (3) the time elapsed since $t = 0$. Actually, the best summary statement of isotope geochemistry was given by Paul Gast (Gast, 1960):

> *In a given chemical system the isotopic abundance of ^{87}Sr is determined by four parameters: the isotopic abundance at a given initial time, the Rb/Sr ratio of the system, the decay constant of ^{87}Rb, and the time elapsed since the initial time. The isotopic composition of a particular sample of strontium, whose history may or may not be known, may be the result of time spent in a number of such systems or environments. In any case the isotopic composition is the time-integrated result of the Rb/Sr ratios in all the past environments. Local differences in the Rb/Sr will, in time, result in local differences in the abundance of ^{87}Sr. Mixing of material during processes will tend to homogenize these local variations. Once homogenization occurs, the isotopic composition is not further affected by these processes.*

This statement can, of course, be equally well applied to the other decay systems.

Table 8.2 lists the radioactive decay schemes of principal geologic interest. The usefulness and significance of each of the decay schemes are different and depend on the geochemical behavior of the parent and daughter, the half-life and the abundance of the parent. We will shortly consider the geological significance of each one.

8.3.1 GEOCHRONOLOGY

Geochronology is not our main interest here, but it is one of the most important applications of isotope geochemistry and the two are often closely intertwined. Let's rewrite equation 8.17 in more general terms:

$$R = R_0 + R_{P/D}(e^{\lambda t} - 1) \qquad\qquad 8.18$$

where R_0 is the initial ratio and $R_{P/D}$ is the parent/daughter ratio. Measurement of geologic time is based on this equation or various derivatives of it. First let's consider the general case. Given a measurement of an isotope ratio, R, and a parent daughter ratio, $R_{P/D}$, two unknowns remain in equation 8.18: t and the initial ratio. We can calculate neither from a single pair of measurements. But if we can measure R and $R_{P/D}$ on a second system for which we believe t and R_0 are the same, we have two equations and two unknowns and subtracting the two equations yields:

$$\Delta R = \Delta R_{P/D}(e^{\lambda t} - 1) \qquad\qquad 8.19$$

which we can solve for t. Rearranging:

$$\frac{\Delta R}{\Delta R_{P/D}} = e^{\lambda t} - 1 \qquad\qquad 8.20$$

t may be then be solved for as:
$$t = \frac{\ln\left(\dfrac{\Delta R}{\Delta R_{P/D}} + 1\right)}{\lambda} \qquad\qquad 8.21$$

We can obtain the ratio $\Delta R/\Delta R_{P/D}$ from any two data points, regardless of whether they are related or not. To overcome this problem in practice, many pairs of measurements of R and $R_{P/D}$ are made. How do we calculate the age when many pairs of measurements are made? Note that equation 8.18 has the form $y = a + bx$, where y is R, a is the intercept, R_0, b is the slope, $e^{\lambda t}$- 1, and x is $R_{P/D}$. An equation of this form is, of course, a straight line on a plot of R vs. $R_{P/D}$, such as Figure 8.6. The slope of the line passing through the data is thus related to the age of the system and is called an *isochron*. When multiple measurements of the daughter isotope ratio and parent-daughter ratio are available, the slope, $\Delta R/\Delta R_{P/D}$, can be calculated the statistical technique of *linear regression*, which we mentioned several times previously, and which is described in Appendix III. The age is then obtained by substituting the value of the slope into equation 8.21. Regression also yields an intercept, which is simply the initial ratio R_0 since, as may

TABLE 8.2: LONG-LIVED RADIOACTIVE DECAY SYSTEMS OF GEOCHEMICAL INTEREST

Parent	Decay Mode	λ	Half-life	Daughter	Ratio
^{40}K	$\beta^+, e.c, \beta^-$	$5.543 \times 10^{-10}\text{y}^{-1}$	$1.28 \times 10^9\text{yr}$	^{40}Ar, ^{40}Ca	^{40}Ar/^{36}Ar
^{87}Rb	β^-	$1.42 \times 10^{-11}\text{y}^{-1}$	$4.8 \times 10^{10}\text{yr}$	^{87}Sr	^{87}Sr/^{86}Sr
^{138}La	β^-	$2.67 \times 10^{-12}\text{y}^{-1}$	$2.59 \times 10^{11}\text{yr}$	^{138}Ce	^{138}Ce/^{142}Ce, ^{138}Ce/^{136}Ce
^{147}Sm	α	$6.54 \times 10^{-12}\text{y}^{-1}$	$1.06 \times 10^{11}\text{yr}$	^{143}Nd	^{143}Nd/^{144}Nd
^{176}Lu‡	β^-	$1.94 \times 10^{-11}\text{y}^{-1}$	$3.6 \times 10^{10}\text{y}$	^{176}Hf	^{176}Hf/^{177}Hf
^{187}Re	β^-	$1.64 \times 10^{-11}\text{y}^{-1}$	$4.23 \times 10^{10}\text{y}$	^{187}Os	^{187}Os/^{186}Os
^{232}Th	α	$4.948 \times 10^{-11}\text{y}^{-1}$	$1.4 \times 10^{10}\text{y}$	^{208}Pb, ^{4}He	^{208}Pb/^{204}Pb, ^{3}He/^{4}He
^{235}U	α	$9.849 \times 10^{-10}\text{y}^{-1}$	$7.07 \times 10^8\text{y}$	^{207}Pb, ^{4}He	^{207}Pb/^{204}Pb, ^{3}He/^{4}He
^{238}U	α	$1.551 \times 10^{-10}\text{y}^{-1}$	$4.47 \times 10^9\text{y}$	^{206}Pb, ^{4}He	^{206}Pb/^{204}Pb, ^{3}He/^{4}He

Note: the branching ratio, i.e. ratios of decays to ^{40}Ar to total decays of ^{40}K is 0.117. The production of ^{4}He from ^{147}Sm decay is insignificant compared to that produced by decay of U and Th.

‡Exact value of λ is in dispute. Recent determinations range from 1.87 to 1.98 x 10^{-11} yr^{-1}.
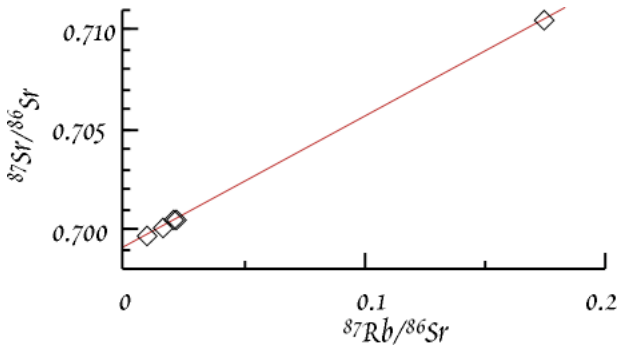
Figure 8.6. A Rb-Sr isochron. Five analyses from a clast in the Bholghati meteorite fall on an isochron, whose slope is related to the age of the system. Data from Nyquist et al. (1990).

be seen from 8.18, $R = R_0$ when $R_{P/D} = 0$.

In special cases, we can calculate t from a single pair of measurements. One such case is where there is no significant amount of the daughter element present at $t = 0$, and we can drop the initial ratio term from equation 8.18. An example is K-Ar dating of volcanic rocks. Ar, the daughter, is lost upon eruption, and the only Ar present is radiogenic Ar. Another example is minerals that concentrate the parent and exclude the daughter. Zircon, for example, accepts U but not Pb; micas accept Rb but not Sr. Even in these cases, however, precise age determination generally requires we make some correction for the very small amounts of the daughter initially present. But since $R >> R_0$, simple assumptions about R_0 generally suffice.

There are two important assumptions built into the use of equation 8.18. (1) The system of interest was at isotopic equilibrium at time $t = 0$. *Isotopic equilibrium in this case means the system had a homogeneous, uniform value of R_0.* (2) The system as a whole and each analyzed part of it was closed between $t = 0$ and time t (usually the present time). Violation of these conditions is the principal source of error in geochronology.

Appendix III sets out the equations for conventional least-squares linear regression. In geochronology, it is important to also make estimates of the error in the age and the error on the initial ratio. These can be estimated from the error on the slope and intercept respectively. However, in practical geochronology, an approach called two-error regression (York, 1969), which takes account of measurement errors in both R and $R_{P/D}$, is generally used. The details of this method are, however, beyond the scope of this book.

8.4 DECAY SYSTEMS AND THEIR APPLICATIONS

8.4.1 Rb-SR

This decay system was one of the first to be widely used in geochronology and remains one of the most useful geochemical tracers. An important advantage of the system is relatively large variations of the Rb/Sr ratio in rocks. Because of the difference in geochemical properties of the two elements, Rb/Sr can vary by several orders of magnitude. Since the accuracy of an age determination depends heavily on the spread of measured ratios, this makes the Rb-Sr system a useful geochronological tool. As we noted in Chapter 7, Rb is a highly soluble, highly incompatible element. Sr is also relatively soluble and is fairly incompatible in mafic and, particularly, ultramafic systems. However, it is relatively compatible in silica-rich igneous systems, partitioning preferentially into plagioclase. The result is that the mantle has a relatively uniform and low $^{87}Sr/^{86}Sr$ ratio, and the continental crust has a much more variable, and, on average, higher ratio.

The Sr isotopic evolution of the Earth and its major silicate reservoirs (the continental crust and mantle) is illustrated in Figure 8.7, which is a plot of $^{87}Sr/^{86}Sr$ vs. time (in giga-annum, or billions of years). Such a plot is called an *isotope evolution diagram*. A characteristic of such diagrams is that a closed reservoir will evolve along a line whose slope is proportional to the parent-daughter ratio, in this case $^{87}Rb/^{86}Sr$. That this is so is easy to show from equation 8.17. Where $t << 1/\lambda$, then equation 8.17 becomes:

$$\frac{^{87}Sr}{^{86}Sr} = \left(\frac{^{87}Sr}{^{86}Sr}\right)_0 + \frac{^{87}Rb}{^{86}Sr}\lambda t \qquad 8.22$$

November 14, 2005

EXAMPLE 8.2. CALCULATING ISOCHRONS AND AGES

The following $^{87}Rb/^{86}Sr$-$^{87}Sr/^{86}Sr$ data were measured by Nyquist et al. (1990) on a clast within the achondritic meteorite Bholghati. These data are plotted in Figure 8.6. What is the age and error on the age of this clast? What is the initial $^{87}Sr/^{86}Sr$ ratio of the clast and the error on this ratio?
Answer: We can calculate the age using equation 8.21 above. The value of $\Delta R/\Delta R_{P/D}$ is the 'slope' of the isochron, i.e., the slope of a line through the data on a plot of $^{87}Sr/^{86}Sr$ vs. $^{87}Rb/^{86}Sr$. We will use simple least squares linear regression to obtain the slope and intercept; the latter will be the initial $^{87}Sr/^{86}Sr$ ratio.

$^{87}Rb/^{86}Sr$	$^{87}Sr/^{86}Sr$
0.01015	0.69966
0.17510	0.71052
0.02166	0.70035
0.02082	0.70029
0.01503	0.69988

Least squares regression is a calculation intensive procedure. Many computer programs are available for calculating regression, and regression functions are built into some hand calculators. Some spreadsheets, such as Microsoft Excel™, also have built in regression functions. However, to illustrate the procedure, we will use a spreadsheet to calculate regression using basic spreadsheet functions and the equations in Appendix III.

Our spreadsheet is shown at left. To make it easier to read, we have defined names for those cells containing calculated parameters; the names are show to the left of the cell. We first calculate the parameters that we will need to use several times in our equations. These are the mean of x and y, the number of values, n, the sum of squares of x and y (Σx_i^2, Σy_i^2) and the sum of the cross products, $\Sigma_{x_iy_i}$. From these parameters, we also calculate the sum of squares of deviations for x ($\Sigma x_i^2 - \bar{x}^2 n$). From these parameters, it is fairly straightforward to calculate the slope, *b*, the intercept, *a*, and the errors on the slope and intercept. Our result is that the age of the clast is 4.57±0.02 Ga (Ga is the abbreviation for gigayears, 10^9 years). At that time, the $^{87}Sr/^{86}Sr$ ratio of the clast was 0.69892±0.00003.

	87Rb/86Sr		87Sr/86Sr	
	0.01015		0.69966	
	0.1751		0.71052	
	0.02166		0.70035	
	0.02082		0.70029	
	0.01503		0.699876	
meanx	0.048552	meany	0.702139	
n	5			
SSQx	0.031892	SSQy	2.465085	
CP	0.171782			
SSQDev	0.020105	(SSQX-x-bar^2*n)		
b	0.066204	(CP-meanx*meany*n)/SSQDev		
a (initia	0.69892	meany-b*meanx		
sigma b	0.000320	SQRT(((SSQy-meany^2*n)		
		-(CP-meanx*meany*n)^2/SSQDev)		
		1/(SSQDev(n-2)))		
sigma a	0.000026	SQRT(((SSQy-meany^2*n)		
		-(CP-meanx*meany*n)^2/SSQDev)		
		*((1/n)+meanx^2/SSQDev)*1/(n-2))		
t	4.57237	±	0.0228	Ga

This equation has the form: $^{87}Sr/^{86}Sr = a + bt$

i.e., the equation of a straight line on a plot of $^{87}Sr/^{86}Sr$ vs. *t* with slope λ $^{87}Rb/^{86}Sr$ and intercept $(^{87}Sr/^{86}Sr)_0$ (to the degree that the Taylor Series approximation is not exact, the line will actually be curved, but the approximation is fairly good in this case). In Figure 8.7 we have plotted geologic age rather than the time since $t = 0$; in other words, we have transformed *t* to (4.55-*t*), where 4.55 Ga is the assumed age of the Earth. Thus the intercept occurs at *t* = 4.55 rather than 0.

The initial $^{87}Sr/^{86}Sr$ ratio of the Earth can be estimated from the initial ratio in meteorites under the assumption that the entire solar system had a uniform $^{87}Sr/^{86}Sr$ at the time it formed. Once it forms, the Earth is a closed system, so it evolves along a straight line with slope proportional to the bulk Earth $^{87}Rb/^{86}Sr$. This ratio has been estimated in various ways to be about 0.085 (as we noted, the $^{87}Rb/^{86}Sr$ is proportional to the Rb/Sr ratio; the bulk Earth Rb/Sr is about 0.029).

Now suppose that a portion of the mantle partially melts at 3.8 Ga to form a segment of continental crust. The new crust has a higher Rb/Sr ratio than the mantle because Rb is more incompatible than Sr. Thus, this crust evolves along a steeper line than the bulk Earth. The residual mantle is left with a
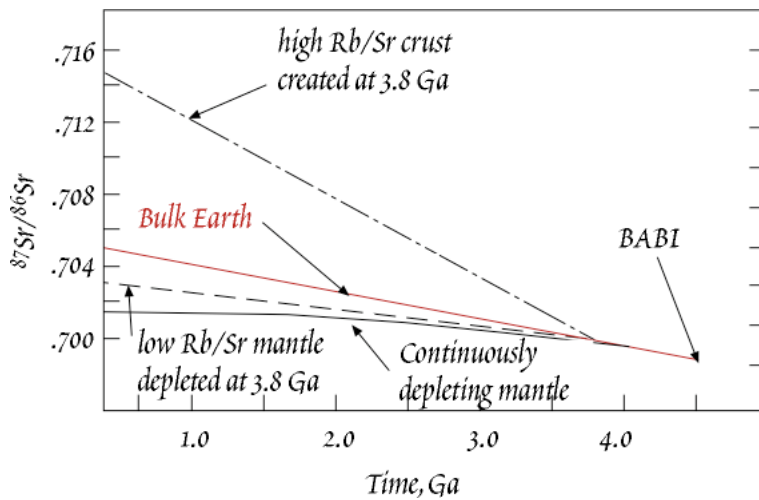
Figure 8.7. Sr isotopic evolution of the bulk Earth, evolution of high Rb/Sr crust created at 3.8 Ga, evolution of the resulting residual mantle and the evolution of a mantle being continuously depleted. 'BABI' stands for basaltic achondrite best initial, and is the assumed initial $^{87}Sr/^{86}Sr$ of the solar system.

lower Rb/Sr ratio than the bulk Earth, and evolves along a shallow slope. If the melting in the mantle and creation of crust were a continuous process, the mantle would evolve along a continuously decreasing slope, i.e., a concave downward path.

The relative mobility of these elements, particularly Rb, can be a disadvantage for geochronology because the closed system assumption is violated. Even very young rocks can be contaminated during weathering, hydrothermal activity, etc. Mobility of Rb or Sr can result in imprecise ages or incorrect initial ratios. On the other hand, the large range in Rb/Sr ratios in siliceous igneous and metamorphic rocks means that Rb-Sr ages are somewhat insensitive to variations in initial $^{87}Sr/^{86}Sr$ ratios.

Because Rb is volatile, we can only guess at the Rb/Sr ratio of the Earth. The present-day chondritic $^{87}Sr/^{86}Sr$ ratio is about 0.725 whereas the $^{87}Sr/^{86}Sr$ ratio of the Earth is thought to be around 0.705.

8.4.2 Sm-Nd

^{143}Nd is produced by α-decay of ^{147}Sm. The Sm-Nd system is in many ways opposite of the Rb-Sr system. First, the Sm/Nd ratio of the mantle is higher than that of the crust and hence the $^{143}Nd/^{144}Nd$ ratio is higher in the mantle than in the crust. Second, the Sm/Nd ratio of the crust and siliceous igneous rocks are relatively uniform, making this system unsuitable for dating such rocks, but variable in mafic and ultramafic rocks (the opposite is true of Rb/Sr). Third, neither Sm nor Nd is particularly mobile, so ages and initial ratios are relatively insensitive to weathering and metamorphism. Fourth, Nd has a short seawater residence time and $^{143}Nd/^{144}Nd$ is not uniform in seawater.

One interesting and useful feature of this system arises from the long residence time of Sr in seawater and its easy substitution in calcium carbonate. Because of its long residence time, the $^{87}Sr/^{86}Sr$ r ratio of seawater is homogeneous at any given time. It does vary with time, however, as is shown in Figure 8.8. The $^{87}Sr/^{86}Sr$ ratio of seawater is controlled by the relative input of Sr from the continents and ridge-crest hydrothermal activity. The ratio of these will vary with mean spreading rate, erosion rates, and plate geometry. The variation of $^{87}Sr/^{86}Sr$ in seawater through the Phanerozoic has been determined from the analysis of carbonate and phosphate fossils, so that ages can be determined simply by determining the $^{87}Sr/^{86}Sr$ ratio of carbonate precipitated from seawater. This is particularly true of the Tertiary, where evolution of $^{87}Sr/^{86}Sr$ in seawater has been particularly precisely determined and there has been a rapid and steady rise in $^{87}Sr/^{86}Sr$.
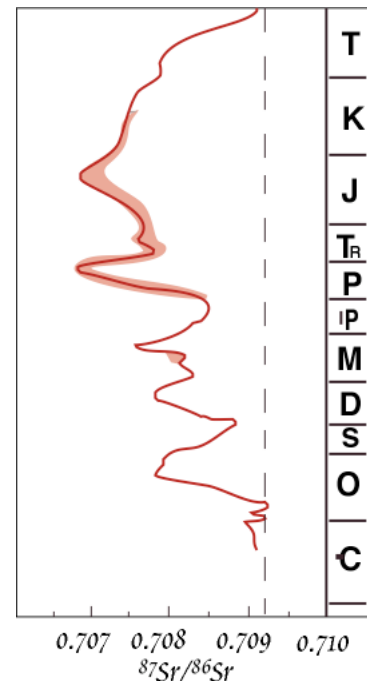

Figure 8.8. $^{87}Sr/^{86}Sr$ in seawater through Phanerozoic time determined from the analysis of phosphate and carbonate fossils. Dashed line shows the composition of modern seawater, grayed areas represent uncertainties.

The Sm/Nd ratio of the bulk Earth can be assumed to be the same as in chondritic meteorites (see Chapters 10 and 11). From the bulk Earth Sm/Nd ratio, the $^{143}Nd/^{144}Nd$ ratio of the bulk Earth can be calculated. That being the case, it is often more meaningful to consider variations in $^{143}Nd/^{144}Nd$ relative to the bulk Earth, or chondritic, value. This is the purpose of ε notation. ε_{Nd} is simply the relative deviation of the $^{143}Nd/^{144}Nd$ ratio from the chondritic ratio in parts in 10^4:

$$\varepsilon_{Nd} = \frac{(^{143}Nd/^{144}Nd) - (^{143}Nd/^{144}Nd)_{chon}}{(^{143}Nd/^{144}Nd)_{chon}} \times 10^4 \qquad\qquad 8.23$$

the present-day chondritic value of $^{143}Nd/^{144}Nd$ is 0.512638 (when corrected for mass fractionation to a $^{146}Nd/^{144}Nd$ ratio of 0.7219). An additional value of the ε_{Nd} notation is that most rocks will have ε_{Nd} values in the range of –20 to +10, and it is certainly easier to work with a one or two digit number than a five or six digit one. Furthermore, we learn something about the history of a rock just by knowing whether its ε_{Nd} is positive or negative. A negative value of ε_{Nd} implies that on average over the history of the Earth the Sm/Nd ratio of that rock or its precursors has been lower than chondritic. This in turn implies the rare earth pattern of the rock or its precursors was light rare earth-enriched. We can draw the opposite inference from a positive ε_{Nd} value. It is often useful to compare the $^{143}Nd/^{144}Nd$ of some ancient rock with the bulk Earth value at the time of its formation, i.e., it's initial $^{143}Nd/^{144}Nd$ or ε_t. We can calculate ε_t simply by substituting the chondritic value appropriate to that time into equation 8.23.

Figure 8.9a illustrates the gross features of the Nd isotope evolution of the Earth. The Earth as a whole has a $^{147}Sm/^{144}Nd$ ratio identical to that of chondrites (0.1967), and the initial $^{143}Nd/^{144}Nd$ of the Earth is also the same as that of chondrites. Thus the bulk Earth evolves along the same line as chondrites. Because Nd is more incompatible than Sm and will therefore be more enriched in a partial melt than Sm, the crust, formed by partial melting of the mantle, has a low Sm/Nd ratio and evolves along a line of lower slope than the bulk Earth. Partial melting depletes the mantle more in Nd than in Sm, so the mantle is left with a high Sm/Nd ratio and evolves along a steeper slope.

By replacing $^{143}Nd/^{144}Nd$ with ε_{Nd} we do not change the fundamental features of the isotope evolution diagram, but the slopes change (Figure 8.9b). Because at any time, ε_{Nd} is the deviation from chondritic $^{143}Nd/^{144}Nd$, the bulk Earth, as well as chondritic meteorites always have $\varepsilon_{Nd} = 0$. Thus they evolve along a line with slope 0. Crustal rocks, with low Sm/Nd, evolve along negative slopes and the mantle, with high Sm/Nd, evolves along a positive slope.
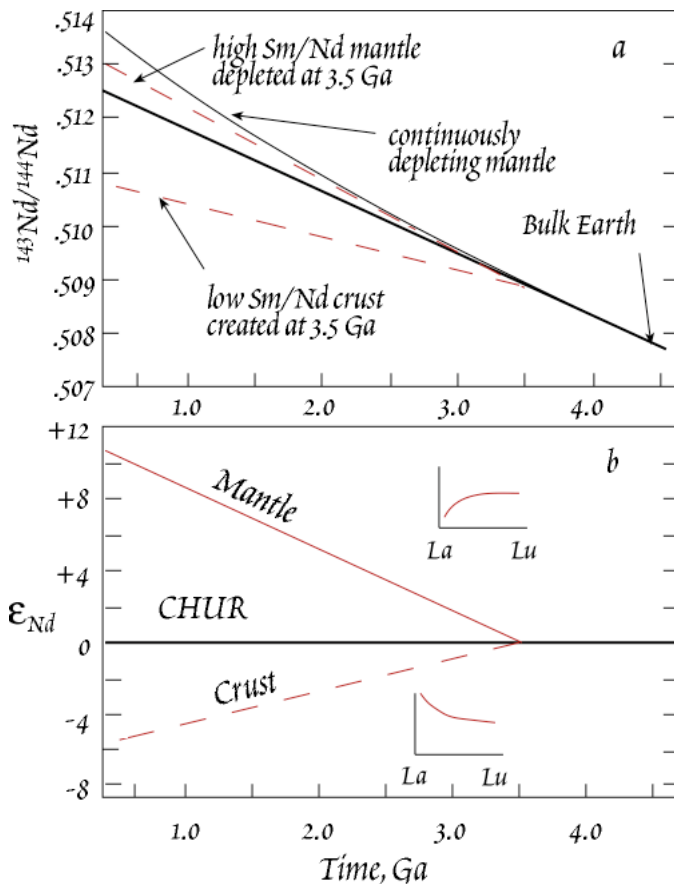
Figure 8.9. (a) Nd isotope evolution in mantle and crust. Bold line shows the evolution of the bulk earth or CHUR (chondritic uniform reservoir); also shown is the evolution of crust created at 3.5 Ga, the corresponding residual mantle, and the evolution of a continuously depleted mantle. (b) Evolution of bulk earth, crust, and mantle when $^{143}Nd/^{144}Nd$ is transformed to ε_{Nd}.

A relatively large fractionation of Sm/Nd is involved in crust formation. But after a crustal rock is formed, its Sm/Nd ratio tends not to change (indeed the ^{147}Sm/^{144}Nd ratio of most crustal rocks is uniform at around 0.13). This leads to another useful concept, the *model age* or *crustal residence time*. Given

---

EXAMPLE 8.3. CALCULATING Nd MODEL AGES

DePaolo (1981) reported that the Pike's Pike granitic batholith has a ^{147}Sm/^{144}Nd ratio of 0.1061 and a ^{143}Nd/^{144}Nd of .51197. What are it's CHUR model and depleted mantle model ages?

Answer: The closed system isotopic evolution of any sample can be expressed as:

$$(^{143}Nd / {}^{144}Nd)_{sam} = (^{143}Nd / {}^{144}Nd)_0 + (^{147}Sm / {}^{144}Nd)_{sam}(e^{\lambda t} - 1) \qquad 8.24$$

The chondritic evolution line is:

$$(^{143}Nd / {}^{144}Nd)_{chon} = (^{143}Nd / {}^{144}Nd)_0 + (^{147}Sm / {}^{144}Nd)_{chon}(e^{\lambda t} - 1) \qquad 8.25$$

The CHUR model age of a system is the time elapsed, $t=\tau$, since it had a chondritic ^{143}Nd/^{144}Nd ratio, assuming the system has remained closed. We can find τ by subtracting equation 8.25 from 8.24:

$$^{143}Nd / {}^{144}Nd_{sam} - {}^{143}Nd / {}^{144}Nd_{chon} = \{^{147}Sm / {}^{144}Nd_{sam} - {}^{147}Sm / {}^{144}Nd_{chon}\}(e^{\lambda t} - 1) \qquad 8.26$$

Another way of thinking about this problem is to imagine a ^{143}Nd/^{144}Nd vs. time plot: on that plot, we want the intersection of the sample's evolution curve with the chondritic one. In terms of the above equations, this intersection occurs at $(^{143}$Nd/^{144}Nd$)_0$.

Solving equ. 8.26 for τ:

$$\tau_{CHUR} = \frac{1}{\lambda} \ln \left(\frac{^{143}Nd / {}^{144}Nd_{sam} - {}^{143}Nd / {}^{144}Nd_{chon}}{^{147}Sm / {}^{144}Nd_{sam} \, {}^{147}Sm / {}^{144}Nd_{chon}} + 1 \right) \qquad 8.27$$

The chondritic ^{143}Nd/^{144}Nd and ^{147}Sm/^{144}Nd ratios are 0.512638 and 0.1967 respectively. Substituting these, the data for the Pike's Pike batholith given above, and λ_{147} from Table 8.2, we have:

$$\tau_{CHUR} = \frac{1}{6.54 \times 10^{-12}} \ln \left(\frac{0.51197 - 0.512638}{0.1061 - 0.1967} + 1 \right) = 1.12 Ga$$

To calculate the depleted mantle model age, τ_{DM}, we use the same approach, but this time we want the intersection of the sample evolution line and the depleted mantle evolution line. So equation 8.27 becomes:

$$\tau_{DM} = \frac{1}{\lambda} \ln \left(\frac{^{143}Nd / {}^{144}Nd_{sam} - {}^{143}Nd / {}^{144}Nd_{DM}}{^{147}Sm / {}^{144}Nd_{sam} \, {}^{147}Sm / {}^{144}Nd_{DM}} + 1 \right) \qquad 8.28$$

The depleted mantle (as sampled by MORB) has an average ε_{Nd} of about 10, or ^{143}Nd/^{144}Nd = 0.51315. The simplest possible evolution path, and the one we shall use, would be a closed system evolution since the formation of the Earth, 4.55 Ga ago (i.e., a straight line on a ^{143}Nd/^{144}Nd vs. time plot). This evolution implies a ^{147}Sm/^{144}Nd of 0.2137. Substituting these values into 8.34:

$$\tau_{DM} = \frac{1}{6.54 \times 10^{-12}} \ln \left(\frac{0.51197 - 0.51315}{0.1061 - 0.2137} + 1 \right) = 1.67 Ga$$

The age of the Pike's Peak batholith has been dated through conventional geochronology as 1.02 Ga (the 'crystallization age'), only slightly younger than the τ_{CHUR}. If we assume the mantle is chondritic in its ^{143}Nd/^{144}Nd and ^{147}Sm/^{144}Nd ratios, then we would conclude that Pike's Peak batholith could have formed directly from mantle-derived material, perhaps by fractional crystallization of basalt. In that case, it represents a new addition of material from the mantle to continental crust. However, DePaolo (1981) pointed out that the mantle has not maintained chondritic ^{143}Nd/^{144}Nd and ^{147}Sm/^{144}Nd ratios, its evolution is more closely approximated by the depleted mantle evolution model described above. Since the τ_{DM} is much older than the crystallization age, he concluded that Pike's Peak batholith originated by melting of pre-existing crustal material; material which had already resided in the crust for some 0.67 Ga before the batholith formed.

---

a measured $^{143}Nd/^{144}Nd$ and $^{147}Sm/^{144}Nd$, and assuming the $^{147}Sm/^{144}Nd$ ratio was constant from the time of formation, we can estimate the 'age' or crustal residence time, i.e., the time the rock has spent in the crust. This assumes we know how the mantle $^{143}Nd/^{144}Nd$ has been evolving with time. A first order assumption is that it evolved like chondrites (i.e., constant $^{147}Sm/^{144}Nd = 0.1967$). Ratios calculated under this assumption are termed chondritic or *CHUR model age* (τ_{CHUR}). More often, a slightly more complex evolution is assumed, in which case the term *depleted mantle model age* is used (τ_{DM}). In either case, the model age is calculated by extrapolating the $^{143}Nd/^{144}Nd$ back to the intersection with the mantle growth curve, as illustrated in Figure 8.10. Example 8.3 illustrates just how such model ages are calculated.

An interesting feature of the behavior of the rare earths is that there is little change in the relative abundances of these elements even in the production of fine-grained sediments from crystalline rocks. This means that meaningful crustal residence ages can be calculated even from sedimentary rocks. The crustal residence age tells how long the sample of Nd has spent in the crust. In other words, a crustal residence time, or age, of 2 Ga measured on particular sediment means the crystalline precursor was derived from the mantle 2.0 by ago. This has led to some interesting inferences about rates of crust formation, which we will discuss later.

Comparatively large variations in Sm/Nd and relatively high Sm/Nd ratios in mafic rocks, and in minerals composing them, make the Sm-Nd decay system a good tool for dating such rocks. The insensitivity of these elements to weathering and metamorphism is an important bonus. On the other hand, the low Sm/Nd ratios of granitic rocks make them unsuitable for Sm/Nd dating. Nevertheless, initial $^{143}Nd/^{144}Nd$ ratios of older rocks have been very useful in tracing the evolution of the crust and mantle. It is now clear that even before 3.5 Ga, the mantle had $^{143}Nd/^{144}Nd$ ratios greater than chondritic (i.e., positive ε_{Nd}). This implies a Sm/Nd greater than chondritic and depletion of the mantle in incompatible elements very early in Earth's history. On the other hand, $^{143}Nd/^{144}Nd$ ratios in the mantle have not increased as rapidly as expected, implying the Sm/Nd ratio of the upper mantle, and perhaps incompatible element concentrations generally, is somehow buffered. We will discuss these issues more fully in a subsequent chapter.

Compared to other parent-daughter ratios, the range in Sm/Nd ratios observed in the Earth is small. That, combined with the long half-life of ^{147}Sm, means that the $^{143}Nd/^{144}Nd$ ratio must be measured to very high precision, with errors no more than 5 parts in 10^5. This level of precision is, however, readily achieved with modern mass spectrometers.

Because of the small range of Sm/Nd ratios, even in mafic rocks, problems can arise in using the Sm-Nd system for geochronology. This small Sm/Nd 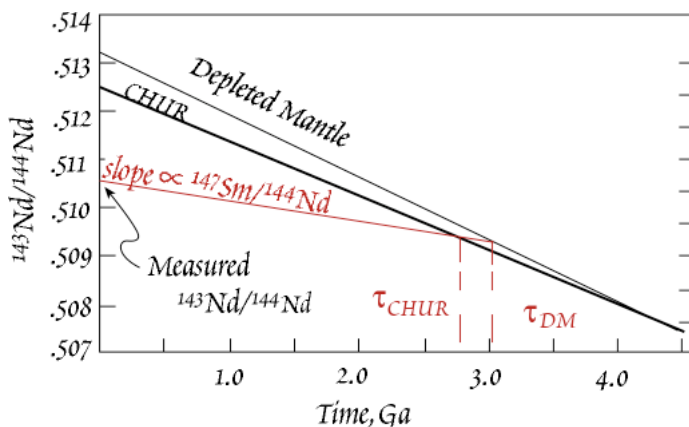range results in a small range in $^{143}Nd/^{144}Nd$ ratios and a calculated age can be influenced by small nonuniformities in the initial $^{143}Nd/^{144}Nd$ ratio. A classic example is the debate that arose over the age of volcanic rocks in Kambalda, Australia. An initial date of 2.7 Ga was obtained by the Sm-Nd technique, but a subsequent study obtained a 3.2 Ga Sm-Nd age. A third study concluded the age was actually 2.7 Ga, and that the 3.2 Ga age resulted from a correlated variation in Sm/Nd and $^{143}Nd/^{144}Nd$ in the rocks at the time of formation (due to assimilation of crust). Zircon and Pb-Pb ages published at about the same time supported this latter interpretation.

Combined use of Sr and Nd isotope ratios can be a particularly powerful geochemical tool. Figure 8.11 shows the Sr and Nd isotopic characteristics of the ma-

Figure 8.10. Sm-Nd model ages. The $^{143}Nd/^{144}Nd$ is extrapolated backward (slope depending on Sm/Nd) until it intersects a mantle or chondritic growth curve. In this example, the *CHUR model age* is 3.05 Ga while the *depleted mantle model age* is 3.3 Ga.

jor terrestrial reservoirs. Sr and Nd isotope ratios tend to be anti-correlated in the mantle and in mantle-derived magmas. This part of the diagram is sometimes called the "mantle array". The inverse correlation reflects the relative compatibilities of the parent-daughter pairs. Rb is less compatible than Sr, while Sm is more compatible than Nd. Thus magmatic processes affect the Rb/Sr and Sm/Nd ratios in opposite ways. In time, this leads to an inverse relationship between $^{87}Sr/^{86}Sr$ and ε_{Nd}. The anti-correlation between Sr and Nd isotope ratios in the mantle reflects the dominance of magmatic processes in the chemical evolution of the mantle. Most of the mantle has ε_{Nd} higher and $^{87}Sr/^{86}Sr$ lower than the bulk Earth. This in turn implies that Sm/Nd ratios have been high and Rb/Sr ratios have been low in the mantle. Mid-ocean ridge basalts (MORB) tend to have lowest $^{87}Sr/^{86}Sr$ and highest ε_{Nd}. This implies the part of the mantle from which MORB is derived must be highly depleted in incompatible elements, presumably through past episodes of partial melting.

The continental crust has, on average, higher $^{87}Sr/^{86}Sr$ and lower ε_{Nd} than the bulk Earth. The anti-correlation between $^{87}Sr/^{86}Sr$ and ε_{Nd} is much weaker in crustal rocks. In part, this reflects the important role of non-magmatic processes have played in evolution of the crust. It also reflects a weaker inverse relationship in Rb/Sr and Sm/Nd in siliceous igneous rocks. The lower continental crust appears to have somewhat lower $^{87}Sr/^{86}Sr$ than does the upper continental crust, but it should be emphasized that there is no clear division in isotopic composition between the two, and that lower crustal rocks may plot anywhere within the crustal field. Continental basalts range to much higher $^{87}Sr/^{86}Sr$ and
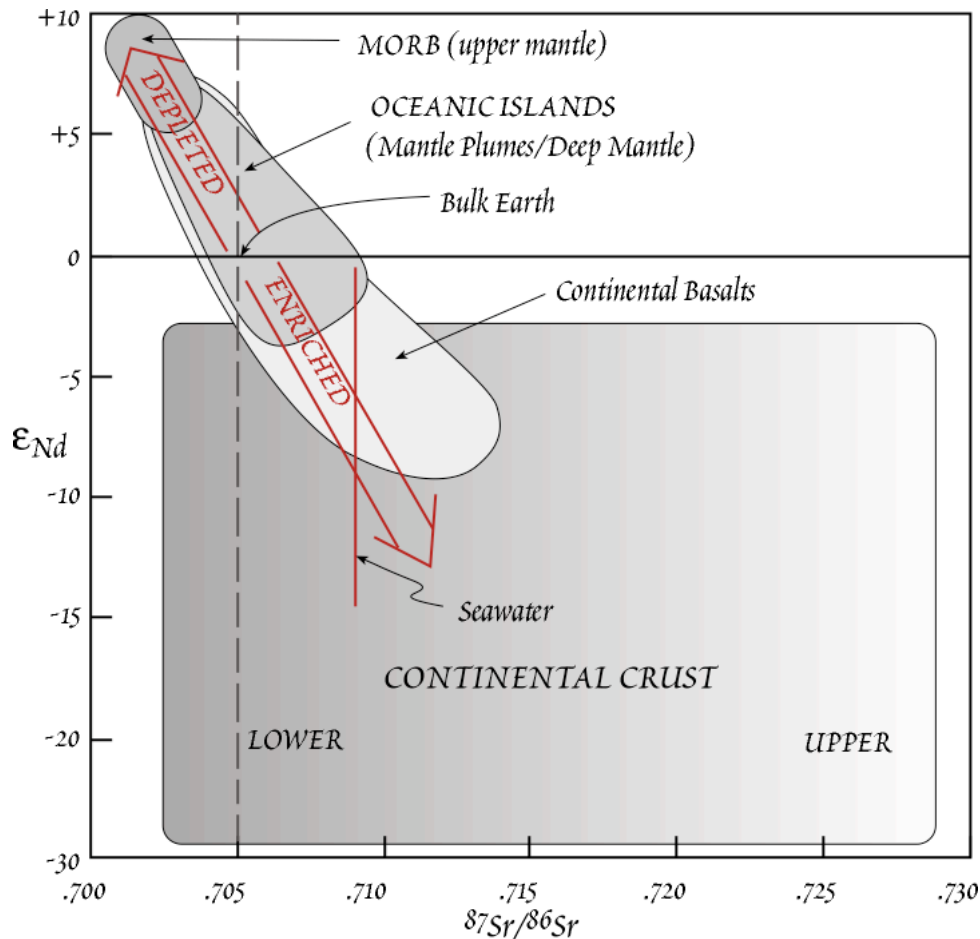

Figure 8.11. Sr and Nd isotope ratios in major geochemical reservoirs. The isotopic composition of the bulk Earth lies at the intersection of the horizontal line at $\varepsilon_{Nd} = 0$ and the dashed vertical line at $^{87}Sr/^{86}Sr = 0.705$ (the latter is dashed because the bulk Earth $^{87}Sr/^{86}Sr$ is somewhat uncertain). Arrows labeled 'enriched' and 'depleted' show where incompatible element enriched and depleted reservoirs would plot.

EXAMPLE 8.4. MODELING THE SR AND ND ISOTOPE EVOLUTION OF THE CRUST AND MANTLE

A simple first order model for the evolution of the crust and mantle might be that the crust was created early in Earth's history by partial melting of the mantle (the mass of the crust is 1.3% that of the mantle). Let's briefly explore the isotopic implications of this model. Assume that the crust was created as a 1.3% equilibrium partial melt of the mantle 3.5 Ga ago. Using partition coefficients of 0.0014, 0.023, 0.194, and 0.0813 for Rb, Sr, Sm, and Nd respectively, calculate the present $^{87}Sr/^{86}Sr$ and $^{143}Nd/^{144}Nd$ of the crust and mantle. Assume that the bulk silicate Earth (i.e., crust plus mantle) $^{87}Rb/^{86}Sr$ and $^{147}Sm/^{144}Nd$ ratios are 0.085 and 0.1967 respectively, and that the bulk silicate Earth $^{87}Sr/^{86}Sr$ and $^{143}Nd/^{144}Nd$ ratios are at present 0.705 and 0.512638 respectively. Also assume that the silicate Earth evolved as a single, uniform, closed system up to 3.5 Ga.

Answer: The first step is to calculate the Rb/Sr and Sm/Nd fractionations during partial melting. Using equation 7.42, we find that the Rb, Sr, Sm, and Nd concentrations in the melt (the crust) are 67.2, 30.2, 4.98, and 10.72 times those in the original source respectively. Since D = C^s/C^ℓ, we calculate the (relative) concentrations in the residual solid (the mantle) by multiplying the melt concentrations by the partition coefficients. From these, we calculate the Rb/Sr and Sm/Nd ratios in the melt to be respectively 2.22 and 0.0465 times those in the original source; these ratios in the residual solid are respectively 0.132 and 1.11 times those in the original source. Multiplying these values times the bulk silicate Earth Rb/Sr and Sm/Nd, we obtain $^{87}Rb/^{86}Sr$ and $^{147}Sm/^{144}Nd$ ratios in the crust of 0.1892 and 0.0914 respectively; those in the mantle are 0.0113 and 0.2184 respectively.

The next step is to calculate the initial ratios at 3.5 Ga. We can calculate the initial ratios at 3.5 Ga by noting that the bulk silicate Earth is still a closed system and hence by solving equation 8.18 for R_0 at t = 3.5 Ga and substituting the values given above for bulk silicate earth parent/daughter ratios and the decay constants in Table 8.2. Doing this, we find the initial ratios (at 3.5 Ga) to be 0.7007 for $^{87}Sr/^{86}Sr$ and 0.5081 for $^{143}Nd/^{144}Nd$. Finally, we calculate present ratios for crust and mantle using equation 8.18 using these initial ratios and the $R_{P/D}$ ratios we calculated above. In this way, we find present $^{87}Sr/^{86}Sr$ ratios of 0.7103 and 0.7012 for the crust and mantle respectively, and present $^{143}Nd/^{144}Nd$ ratios of 0.5102 and 0.5131 for crust and mantle respectively.

---

lower ε_{Nd} than do oceanic basalts. For the most part, this is due to assimilation of continental crust by these magmas. In some cases, however, it may reflect derivation of these magmas from incompatible element enriched regions of the subcontinental mantle.

Because $^{143}Nd/^{144}Nd$ ratios are not uniform in seawater, $^{143}Nd/^{144}Nd$ ratios in ancient sediments cannot be used for dating the way $^{87}Sr/^{86}Sr$ ratios are. However, $^{143}Nd/^{144}Nd$ ratios have been used to identify different water masses and to attempt to constrain ocean circulation.

8.4.3 Lu-Hf

The Lu-Hf system is in many respects similar to the Sm-Nd system: (1) in both cases both elements are relatively immobile; (2) in both cases both elements are refractory so we can assume the bulk silicate earth has a Lu/Hf ratio close to chondritic; (3) in both cases the daughter is preferentially enriched in the crust so both $^{143}Nd/^{144}Nd$ and $^{176}Hf/^{177}Hf$ ratios are lower in the crust than in the mantle.

Because of (2), we can usefully define an ε_{Hf}, which is the relative deviation in parts in 10^4 from the chondritic value. ε_{Hf} is calculated as

$$\varepsilon_{Hf} = \frac{^{176}Hf/^{177}Hf - {^{176}Hf/^{177}Hf_{chon}}}{^{176}Hf/^{177}Hf_{chon}} \times 10^4 \qquad 8.29$$

The present-day chondritic value is about 0.28280±0.00003: the exact value is still disputed.

The correlation between Nd and Hf isotope ratios in mantle-derived rocks is somewhat better than between Sr and Nd isotope ratios, as one might expect from the chemical behavior of the elements in-

volved: Lu is after all a rare earth like Sm and Nd, and the behavior of Hf is somewhat similar to that of the rare earths. The fractionation of Lu from Hf tends to be somewhat greater than between Sm and Nd and as a result there is greater variation in $^{176}Hf/^{177}Hf$ than in $^{143}Nd/^{144}Nd$. Figure 8.11 shows how Hf isotope ratios relate to Sr and Nd isotope ratios in oceanic basalts. Hf and Nd isotope ratios scatter about a trend of $\varepsilon_{Hf} = 1.4 \times \varepsilon_{Nd}$, as is illustrated in Figure 8.12.

Because they vary more, Hf isotope ratios should be a better geochemical tool than Nd isotope ratios, at least in principle. However, Hf is a difficult element to analyze in conventional thermal ionization mass spectrometers because it does not ionize readily. Until the development of multi-collector inductively coupled plasma mass spectrometers (MC-ICP-MS), which utilize an Ar plasma for ionization, the difficulty of analysis of Hf isotope ratios meant that few such measurements were made. In the last decade, however, increasing use of the Lu-Hf system has been made in both isotope geochemistry and geochronology. However, some disadvantages relative to the Sm-Nd system remain. Among these are difficulties in establishing the Lu/Hf ratio of the Earth, uncertainty about the present day chondritic value as mentioned above, and even uncertainty as to the exact value of the decay constant. These are all topics of active current research.

In the sedimentary reservoir, the similarity of the Lu-Hf and Sm-Nd systems breaks down. This is because Hf is geochemically very similar to Zr and as a result is concentrated in zircon in crustal rocks. Zircon is very stable mechanically and chemically and concentrates in coarse-grained sediments. Rare earths, including Lu tend to be more concentrated in fine-grained clays. As a result, Hf and Nd isotope ratios are not correlated in sedimentary rocks (e.g., Patchett et al., 1984; White et al., 1986).
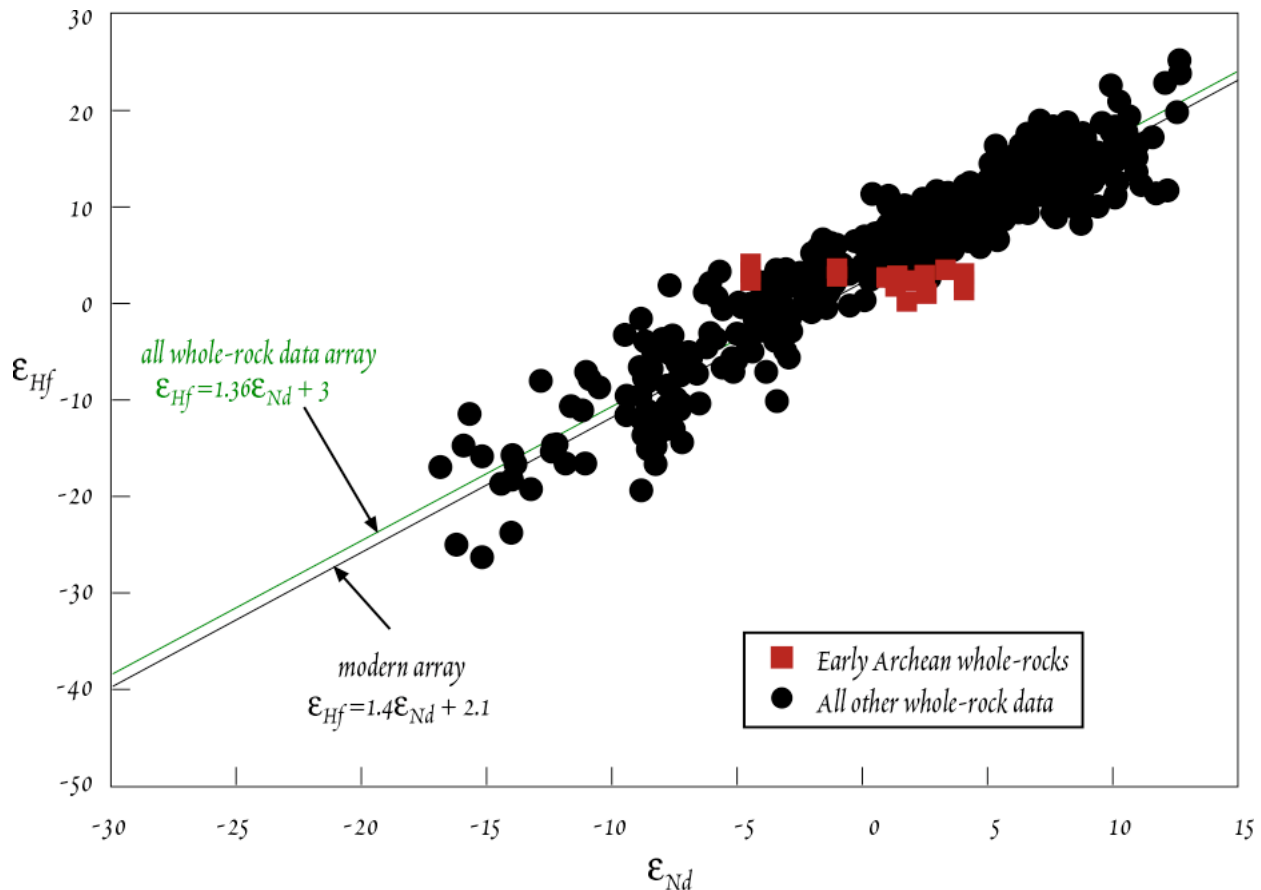

Figure 8.12. ε_{Hf} vs. $^{87}Sr/^{86}Sr$ and ε_{Nd} in MORB and oceanic island basalts.

8.4.4 Re-Os

^{187}Re decays to ^{187}Os by β^- decay with a half-life of 42 billion years. Unlike the other decay systems of geological interest, Re and Os are both siderophile elements. Thus, they are depleted in the silicate Earth by about 2 orders of magnitude compared to chondritic meteorites. The missing Re and Os are presumably in the core. The resulting very low concentration levels (sub-ppb) make analysis extremely difficult. Although the first Re-Os isotope studies were published in the early 1960's, isotopic analysis of Os proved so difficult that there were no follow-up studies until 1980, when an analysis technique using the ion probe was developed (Luck et al., 1980). However, it was not until the development of a new analytical technique (Creaser et al., 1991), which employed a conventional thermal ionization mass spectrometer to analyze OsO_4^-, that interest in this system really blossomed.

Several aspects of this decay system make it particularly useful in addressing a variety of geological processes. The first is the siderophile/chalcophile nature of these elements, making this a useful system to address questions of core formation and ore genesis. Second, whereas all the other radioactive and radiogenic elements are incompatible ones, and hence enriched in melts, Os is a highly compatible element (bulk D ~ 10) and is enriched in the residual solid. This makes Os isotope ratios particularly useful in studies of the mantle. Third, while Os is highly compatible, Re is moderately incompatible and is slightly enriched in the melt. For example, mantle peridotites have average Re/Os close to the chondritic value of 0.08 whereas the average Re/Os in basalts is 8.9. Thus partial melting appears to produce an increase in the Re/Os ratio by a factor of ~10^2. As a consequence, the range of Os isotope ratios in the Earth is enormous compared to other radiogenic elements (thus analytical precision need not be as high as for elements such as Sr, Nd, and Hf). The mantle has a ^{187}Os/^{188}Os ratio close to the chondritic value of 0.1275 (Allègre and Luck, 1980), whereas the crust appears to have a Re/Os isotope ratio of 1.2 to 1.3 (Esser and Turekian, 1993). By contrast, the difference in ^{143}Nd/^{144}Nd ratios between crust and mantle is only about 0.5%.
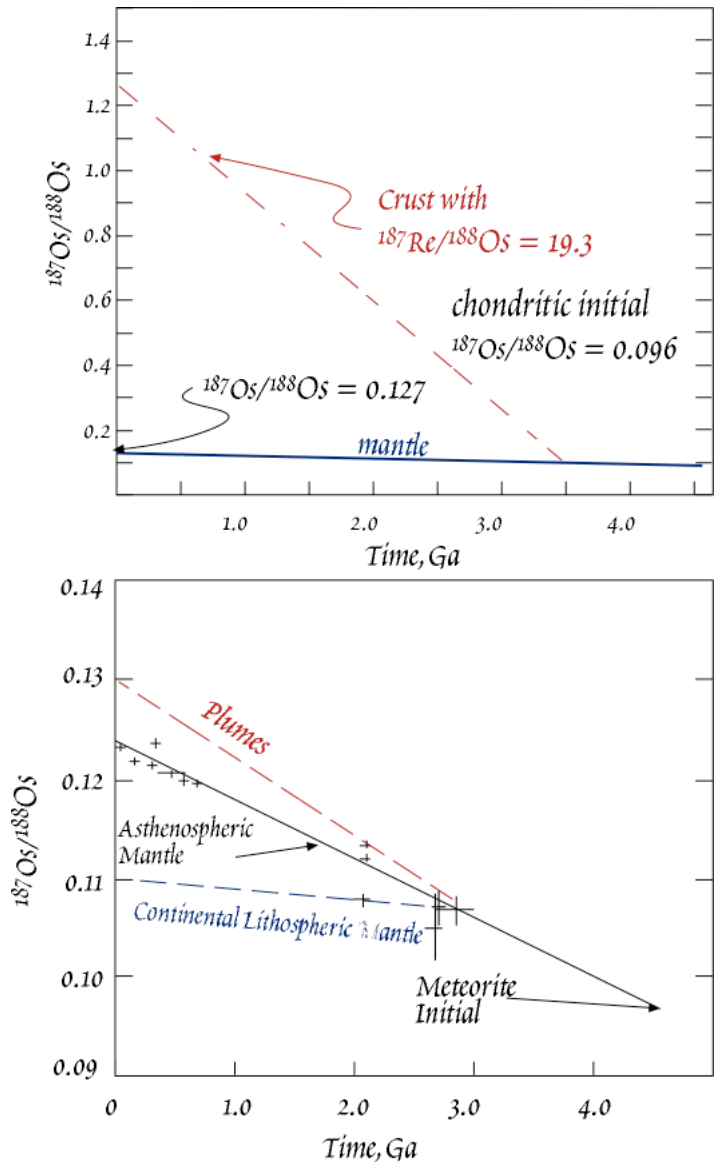

Figure 8.13. a.) Schematic evolution of Os isotope ratios in the mantle and crust. b.) ^{187}Os/^{188}Os evolution in the mantle as deduced from analyses of osmiridum and laurite grains in ancient mantle peridotites, initial ratios in peridotites, and modern oceanic peridotites and basalts. The pattern is consistent with other isotopic systems: The asthenospheric mantle is more incompatible element-depleted than mantle plumes, which produced oceanic island basalts. The mantle root of continents (lithospheric mantle), appears to have been severely depleted of its basaltic component and Re by melt extraction.
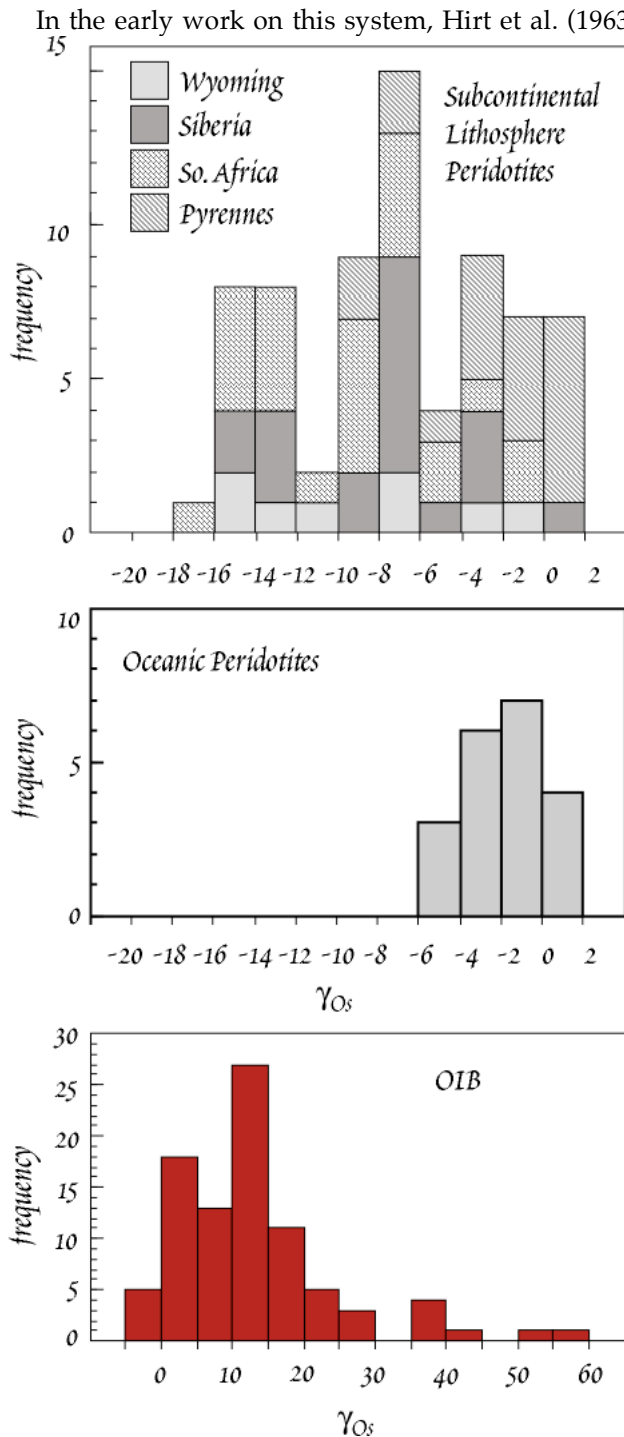
In the early work on this system, Hirt et al. (1963)

Figure 8.14. Histogram comparing γ_{Os} in peridotites of the subcontinental lithosphere, the upper oceanic mantle and oceanic island basalts (OIB). Samples from subcontinental lithosphere typically have γ_{Os} of -10, those of the oceanic upper mantle are typically -2. OIB average γ_{Os} of +10. Those OIB with the most extreme γ_{Os} may have assimilated oceanic crust during eruption.

reported the isotope ratio as $^{187}Os/^{186}Os$ (normalized for fractionation to $^{192}Os/^{188}Os$ of 3.08271). However, ^{186}Os is itself radiogenic, being the product of α-decay of ^{190}Pt. ^{190}Pt is sufficiently rare, and its half-life sufficiently long, that in most cases the amount of radiogenic ^{186}Os is insignificant. Significant radiogenic ^{186}Os was, however, observed by Walker et al. (1991) in copper ores from Sudbury, Ontario, which prompted them to adopt the convention of using ^{188}Os as the normalizing isotope. Eventually, this convention was adopted by other laboratories as well and today Os isotope ratios are reported as $^{187}Os/^{188}Os$, but there is a considerable amount of data in the literature using the old convention. $^{187}Os/^{186}Os$ ratios may be converted to $^{187}Os/^{188}Os$ ratios by multiplying by 0.12035.

Perhaps the first significant result from Re-Os studieswas the realization the Re/Os ratio of the mantle is nearly chondritic (Allègre and Luck, 1980). This is a bit surprising if most of Re and Os have been extracted to the core. If the core and mantle are in equilibrium, then mantle concentrations will be determined by metal-silicate partition coefficients, which are large for both elements. Since the partition coefficients of these two elements are different, the ratio of the two in the mantle should be quite different from chondritic. That the Re/Os ratio of the mantle is chondritic thus has important implications for how and when the core formed, which we will discuss in Chapter 11. Figure 8.13 illustrates the evolution of Os isotope ratios in the crust and mantle.

Since the silicate Earth appears to have a near-chondritic $^{187}Os/^{188}Os$ ratio, it is useful to define a parameter analogous to ε_{Nd} and ε_{Hf} that measures the deviation from chondritic. Walker et al. (1989) defined γ_{Os} as:

$$\gamma_{Os} = \frac{\frac{^{187}Os}{^{188}Os} - \frac{^{187}Os}{^{188}Os}_{Chon}}{^{187}Os/^{188}Os_{Chon}} \times 100 \qquad 8.30$$

where the present day chondritic value is 0.12753. Thus γ_{Os} is the *percent* deviation from the chondritic value. Just as with ε_{Nd}, we can calculate values of γ_{Os} for times other than the present by using initial $^{187}Os/^{188}Os$ and an chondritic value appropriate to that time.

It is important to remember that, unlike the Sm-Nd and Lu-Hf systems, there is no reason to believe that the Re/Os and $^{187}Os/^{188}Os$ ratios of the silicate Earth are *exactly* chondritic. Observa-

tional evidence suggests the $^{187}Os/^{188}Os$ is within a few percent of the chondritic value, but more than that cannot be said.

Because of the extremely low concentrations of Os in most rocks, most early studies of Os isotope ratios focused on analysis of Os-rich grains, such as osmiridium alloy and laurite (RuS_2) in peridotites. Improvement in analytical techniques eventually allowed the analysis of peridotites and other ultramafic rocks such as komatiites, and Os-rich sediments such as black shales and Mn nodules, where Os concentrations exceed a part per billion. Although it remains analytically challenging, the negative ion method of Creaser et al. (1991) allows the analysis of basalts and clays with concentrations in the parts per trillion range. Consistent with Sr and Nd isotope systematics, these studies have shown that MORB and related peridotites have lower $^{187}Os/^{188}Os$ ratios than basalts from oceanic islands (e.g., Martin, 1991; Hauri and Hart, 1993; Reisberg et al., 1993). These results are consistent with the Nd and Sr isotope evidence we have already discussed that the source of MORB is more incompatible-element depleted than mantle plumes, which are thought to produce oceanic island volcanoes such as Hawaii. However, MORB typically have higher $^{187}Os/^{188}Os$ ratios than peridotites dredged from mid-ocean ridges (so-called abyssal peridotites). This is somewhat surprising since the peridotites are thought to be residual from the melting that produces MORB. If isotopic equilibrium is achieved, both should have the same isotope ratio. The difference may mean that isotopic equilibrium is not achieved during partial melting, at least for Os. Alternatively, the difference between MORB and abyssal peridotites could just reflect pervasive contamination of MORB by seawater, which has much higher $^{187}Os/^{188}Os$. The concentration of Os in MORB is extremely low, far lower than in peridotites, meaning relatively small amounts of contamination could shift the isotope ratios.

Another interesting result of Re-Os studies has been the evidence for systematically low $^{187}Os/^{188}Os$ in the subcontinental lithosphere. Studies of pieces of subcontinental mantle carried to the surface as xenoliths in magmas have revealed that much of this mantle is poor in clinopyroxene and garnet and hence depleted in its basaltic component (the term "infertile" is often used to refer to such compositions), presumably as a result of previous episodes of melting. Surprisingly, these xenoliths often show evidence of incompatible element enrichment, including high $^{87}Sr/^{86}Sr$ and low ε_{Nd}. This latter feature is often attributed to reaction of the mantle lithosphere with very small degree melts percolating upward through it (a process termed "mantle metasomatism"). This process, however, apparently leaves the Re-Os system unaffected, so that $^{187}Re/^{188}Os$ and $^{187}Os/^{188}Os$ remain low. Figure 8.14 compares the γ_{Os} values of subcontinental lithosphere, oceanic peridotites (presumably representing the isotopic com-

position of the upper asthenospheric mantle, though to be the source of MORB), and oceanic basalts. Thus Re-Os studies are proving to be important in understanding the evolution of the subcontinental lithosphere, and its role in volcanism. We shall return to these topics in Chapter 11.

There has also been considerable interest in the Os isotope composition of seawater. The $^{187}Os/^{188}Os$ ratio of modern seawater is about seawater is about 8. Like that of $^{87}Sr/^{86}Sr$, $^{187}Os/^{188}Os$ depends on
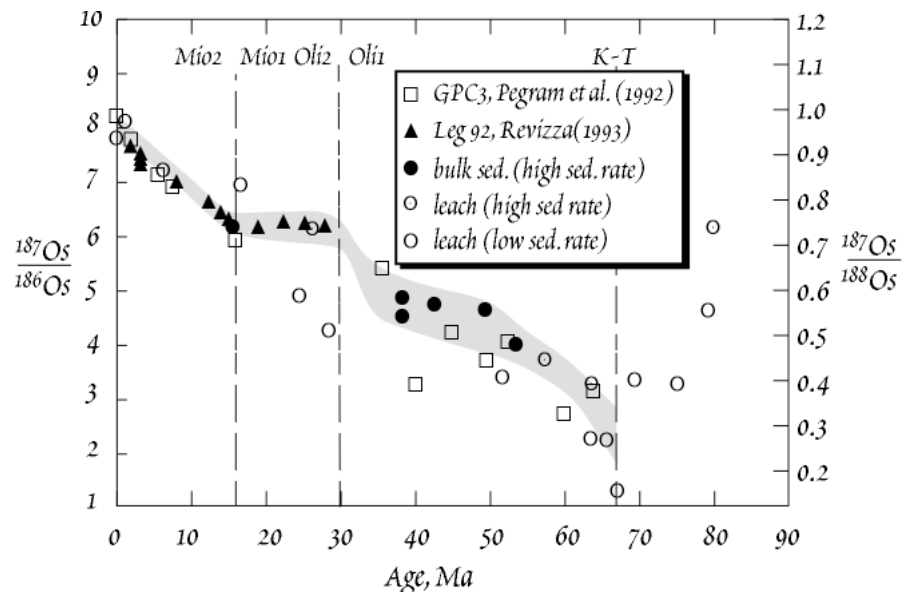

Figure 8.15. Os isotope composition of seawater over the last 80 Ma, from Peuker-Ehrenbrink et al. (1995). Gray field represents the authors best estimates of seawater Os isotopic composition.

the balance of continental fluxes (e.g., rivers, with $^{187}Os/^{188}Os \sim 1.2$) and oceanic crustal fluxes (e.g., hydrothermal activity, with $^{187}Os/^{188}Os \sim 0.13$). In addition, however, cosmic fluxes ($^{187}Os/^{188}Os \sim 0.13$), which include both cosmic dust, which continually settles through the atmosphere into the oceans, and large meteorite impacts, may be significant for Os. Because of the low concentrations of Os in seawater, the Os isotopic composition of seawater cannot be measured directly. It can, however, be measured indirectly by analyzing the authigenic component in seawater, such as Mn nodules and the leachable fraction of clays.

Like Sr, the Os isotopic composition of seawater has changed over time (Figure 8.15). There are obvious similarities between the Os isotopic and Sr isotopic evolution of seawater, most notably the increase of both through the Tertiary period (the last 65 million years). This may in part reflect a decreasing hydrothermal flux resulting from decreasing sea floor spreading rates. There are also differences, which reflect the differing geochemical behavior of Sr and Os. The geochemical behavior of both at the surface of the Earth is related to carbon, but while Sr is concentrated in carbonates, Os is concentrated in organic-rich sediments. The very low Os isotope ratios at the Cretaceous-Tertiary boundary (65 Ma), may reflect a sudden input of meteoritic Os as a result of the impact of a large meteorite that apparently occurred then.

8.4.5 La-Ce

This is another system that is analytically challenging. ^{138}La is a rather rare isotope (an odd-odd), and its long half-life does not help matters. Worse, ^{138}Ce is also a trace isotope of Ce, which would be O.K. except for the problem of analyzing for a very rare isotope in the presence of a very common one (^{140}Ce). Lastly, ^{138}Ba is among the most abundant heavy isotopes (because it has 82 neutrons, a magic number), and can interfere with the analysis.

As Figure 8.16 shows, $^{138}Ce/^{142}Ce$ (or $^{138}Ce/^{136}Ce$, a convention has not evolved) and $^{143}Nd/^{144}Nd$ are negatively correlated. This correlation is exactly what is expected because the parent, La, is more incompatible than the daughter, Ce, but the daughter of the Nd–Sm system is more incompatible than the parent. This leads to an expected anticorrelation between La/Ce and Sm/Nd ratios and, ultimately, between $^{138}Ce/^{142}Ce$ and $^{143}Nd/^{144}Nd$. How well they are correlated is not yet clear.
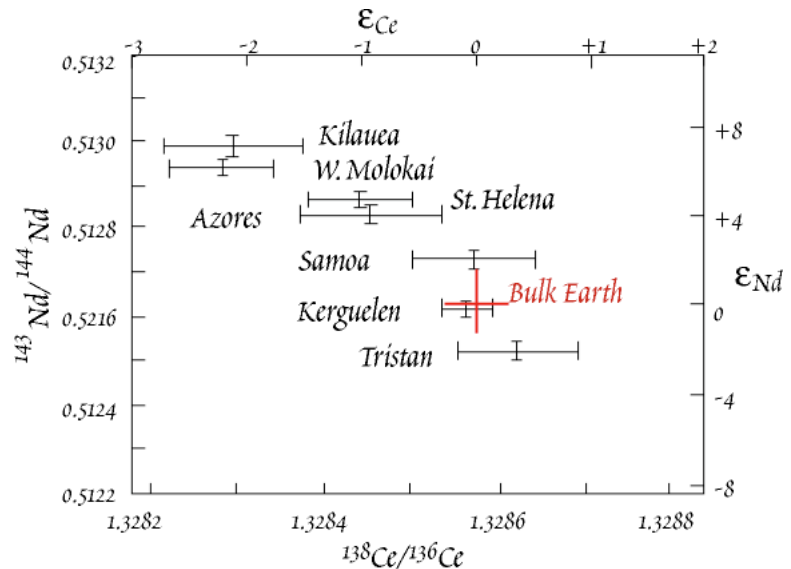

Figure 8.16. Ce and Nd isotope ratios in oceanic basalts (Dickin, 1987)

8.4.6 U-Th-Pb

The U-Th-Pb system is somewhat of a special case since there are 3 decay schemes producing isotopes of Pb. In particular two U isotopes decay to two Pb isotopes, and since the two parents and two daughters are chemically identical, we get two decay systems for the price and one and together they provide a particularly powerful tool.

Let's explore the mathematics of this. Following convention, we will designate the $^{238}U/^{204}Pb$ ratio as μ, and the $^{232}Th/^{238}U$ ratio as μ. The ratio $^{238}U/^{235}U$ is constant in the Earth at 137.88 (except in nuclear reactors and the Oklo deposit mentioned earlier). Now, we can write two versions of equation 8.18:

$$^{207}Pb/^{204}Pb = {}^{207}Pb/^{204}Pb_0 + \frac{\mu}{137.88}(e^{\lambda_{235}t} - 1) \qquad 8.31$$

and
$$^{206}Pb\,/\,^{204}Pb = \,^{206}Pb\,/\,^{204}Pb_0 + \mu(e^{\lambda_{238}t} - 1) \qquad\qquad 8.32$$

Equations 8.31 and 8.32 can be rearranged by subtracting the initial ratio from both sides. For example, using Δ to designate the difference between the initial and the present ratio, equation 8.32 becomes:

$$\Delta\,^{206}Pb\,/\,^{204}Pb = \mu(e^{\lambda_{238}t} - 1) \qquad\qquad 8.33$$

Dividing the equivalent equation for ^{235}U-^{207}Pb by equation 8.33 yields:

$$\frac{\Delta\,^{207}Pb\,/\,^{204}Pb}{\Delta\,^{206}Pb\,/\,^{204}Pb} = \frac{1}{137.88}\frac{(e^{\lambda_{235}t} - 1)}{(e^{\lambda_{238}t} - 1)} \qquad\qquad 8.34$$

The left-hand side of this equation is the slope of line on a plot of $^{207}Pb/^{204}Pb$ vs. $^{206}Pb/^{204}Pb$ such as Figure 8.17. The slope depends only on time and three constants (λ_{238}, λ_{235}, and $^{238}U/^{235}U$). Because its slope depends on time, a line on a plot of $^{207}Pb/^{204}Pb$ vs. $^{206}Pb/204Pb$ is an isochron, analogous to the isochrons in a plot such as Figure 8.6. We derived equation 8.34 by subtracting the initial ratio from the present one, but we could derive the identical equation by subtracting equations for two separate samples that share common initial ratios and time. Equation 8.34 differs from the conventional isochron equation (equation 8.18) in that terms for the initial values and the parent-daughter ratios do not appear. The point is, if we measure the Pb isotope ratios in a series of samples that all started with the same initial isotopic composition of Pb at some time t_0, and which all remained closed to gain or loss of Pb or U since then, we can determine the age of this system without knowing the parent-daughter ratio.

The bad news is that equation 8.34 cannot be solved directly for t. However, we can guess a value of t, plug it into the equation, calculate the slope, compare the calculated slope with the observed one, revise our guess of t, calculate again, etc. Pretty laborious, but using a computer to make 'educated guesses' of t, it is pretty easy. If fact, there are algorithms available that converge to a high degree of accuracy after a few iterations[*]. This kind of isochron is called a Pb-Pb isochron and the age derived from it is called a Pb-Pb age. A disadvantage of Pb-Pb isochrons is that we cannot determine initial ratios from them.

Because the half-life of ^{235}U is much shorter than that of ^{238}U, ^{235}U decays more rapidly. As a result, on a plot $^{207}Pb/^{204}Pb$ vs. $^{206}Pb/^{204}Pb$, Pb isotopic evolution follows curved paths. The exact path that is followed depends upon μ. Three such evolution curves are shown in Figure 8.15. All systems that begin with a common initial isotopic composition at time t_0 along a straight line at some later time t. This line is the Pb-Pb isochron.

As an example, let's consider the various bodies of the solar system. We assume that (and there has been no evidence to the contrary) when the solar system formed 4.55 billion years ago, it had a single, uniform Pb isotope composition, which we will refer to as primordial Pb. Planetary bodies formed shortly after the solar system formed, and we can reasonably assume that they have remained closed since their formation (i.e., they have neither gained nor lost Pb or U). There is no reason to assume that all planetary bodies started with the same ratio of U to Pb, i.e., the same value of μ. Indeed, there is good evidence that they did not. So Pb in each planetary body would evolve along a separate path that would depend on the value of μ in that body. However, at any later time t, the $^{207}Pb/^{204}Pb$ and $^{206}Pb/^{204}Pb$ ratios of all planetary bodies plot on a unique line. This line, called the *Geochron*, has a slope whose age corresponds to the age of the solar system, and it passes through the composition of primordial Pb.

Equation 8.34, in which the parent/daughter ratio term does not appear, turns out to be very useful for several reasons. First, for geochronological applications, U is a rather mobile element, so the closed system assumption is often violated. Often this mobility occurs late (perhaps occurring as the rock is unburied and reaches the surficial weathering zone). So a normal U-Pb isochron often gives erroneous results. But if the loss (or gain) has been sufficiently recent, Pb isotope ratios will not be significantly affected. Because of this, Pb-Pb ages calculated with equation 8.34 are robust with respect to recent mobility of U, and good ages can be obtained this way even when they cannot be obtained from a conventional U-Pb isochron (i.e., from the slope of $^{206}Pb/^{204}Pb$ vs. $^{238}U/^{204}Pb$).

---

[*] This kind of algorithm is available as a standard Add-In call the "Solver" in Microsoft Excel.
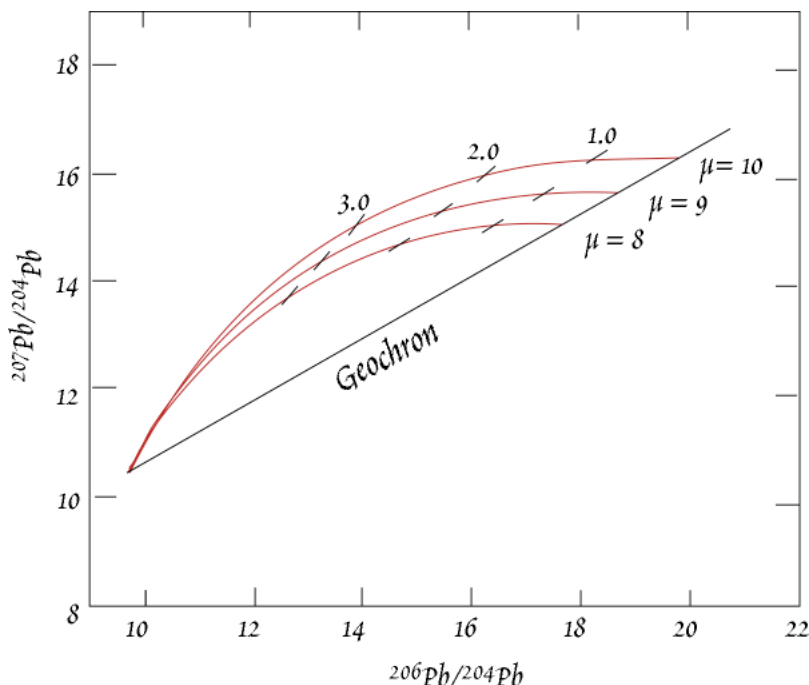
Figure 8.17. Evolution of Pb isotope ratios. The curve lines represent the evolutionary paths for systems having μ values of 8, 9, and 10. The hash marks on the evolution curves mark Pb isotope compositions 1.0, 2.0, and 3.0 Ga ago.

Table 8.3. Initial Isotopic Compositions and Parent-Daughter Ratios for the Earth

System	R_0	$R_{P/D}$*	Source
^{87}Rb-^{87}Sr	0.69898	~0.085	basaltic achondrites
^{147}Sm-^{143}Nd	0.50670	0.1967	chondrites
^{176}Lu-^{176}Hf	0.2797$^{£}$	0.0334	eucrites, chondrites
^{187}Re-^{187}Os†	0.09677	0.397	chondrites
^{187}Re-^{187}Os‡	0.8041	3.299	chondrites
^{235}U-^{207}Pb	10.294	~0.058	Canyon Diablo troilite
^{238}U-^{206}Pb	9.314	~8	Canyon Diablo troilite
^{232}Th-^{208}Pb	29.476	~32	Canyon Diablo troilite

*The parent daughter ratio is given as the present day value.
†Ratios for ^{187}Os/^{188}Os and ^{187}Re/^{188}Os
‡Ratios for ^{187}Os/^{186}Os and ^{187}Re/^{186}Os
$^{£}$Exact value disputed between 0.279628 and 0.279742

A second important application is 'mantle isochrons'. It is reasonable to assume that the isotope ratios in a volcanic rock will be the same as the isotope ratios of its source because the different isotope of an element, for example ^{206}Pb and ^{204}Pb, are chemically identical and cannot be fractionated by magmatic processes (which is to say that their partition coefficients are identical). But isotopes of different elements, for example ^{238}U and ^{206}Pb, are not chemically identical and can be fractionated. Thus the U/Pb or ^{238}U/^{204}Pb ratio of a volcanic rock is not necessarily the same as that of its source. As a result, we cannot calculate an 'age' of the source of a series of volcanic rocks using the normal isochron equation, 8.31 or 8.32. Since the parent-daughter ratio does not occur in equation 8.34, we can calculate an age using equation 8.34. Such 'mantle isochron' ages for oceanic basalt sources are typically 1 to 2 Ga.

We cannot assume that the U-Pb ratio of the Earth is chondritic, indeed the evidence is that it is not. Thus unlike the Sm-Nd and Lu-Hf systems, we don't have any *a priori* constraints on the U/Pb ratio of the Earth. However, assuming the Earth formed at the same time and from the same materials as meteorites, and that it has remained closed to gain or loss of U and Pb, its ^{207}Pb/^{204}Pb and ^{206}Pb/^{204}Pb must fall on the Geochron just like any other planetary body. This applies only to the Earth as a whole. Reservoirs within the Earth, such as the crust and mantle and individual rock units, have clearly not been closed systems for 4.55 Ga, so their isotope ratios need not fall on the Geochron. The mean of all such reservoirs should, however, fall on the Geochron.

The initial isotopic composition of the Earth can be estimated from that in meteorites, as is the case for other isotope systems. Most terrestrial reservoirs do plot fairly close to the Geochron and close to an evolution curve corresponding to a value of μ of about 8. Table 8.3 lists estimated values for the initial isotopic composition of the Earth and solar system, as well as estimated parent/daughter ratios for the bulk Earth.
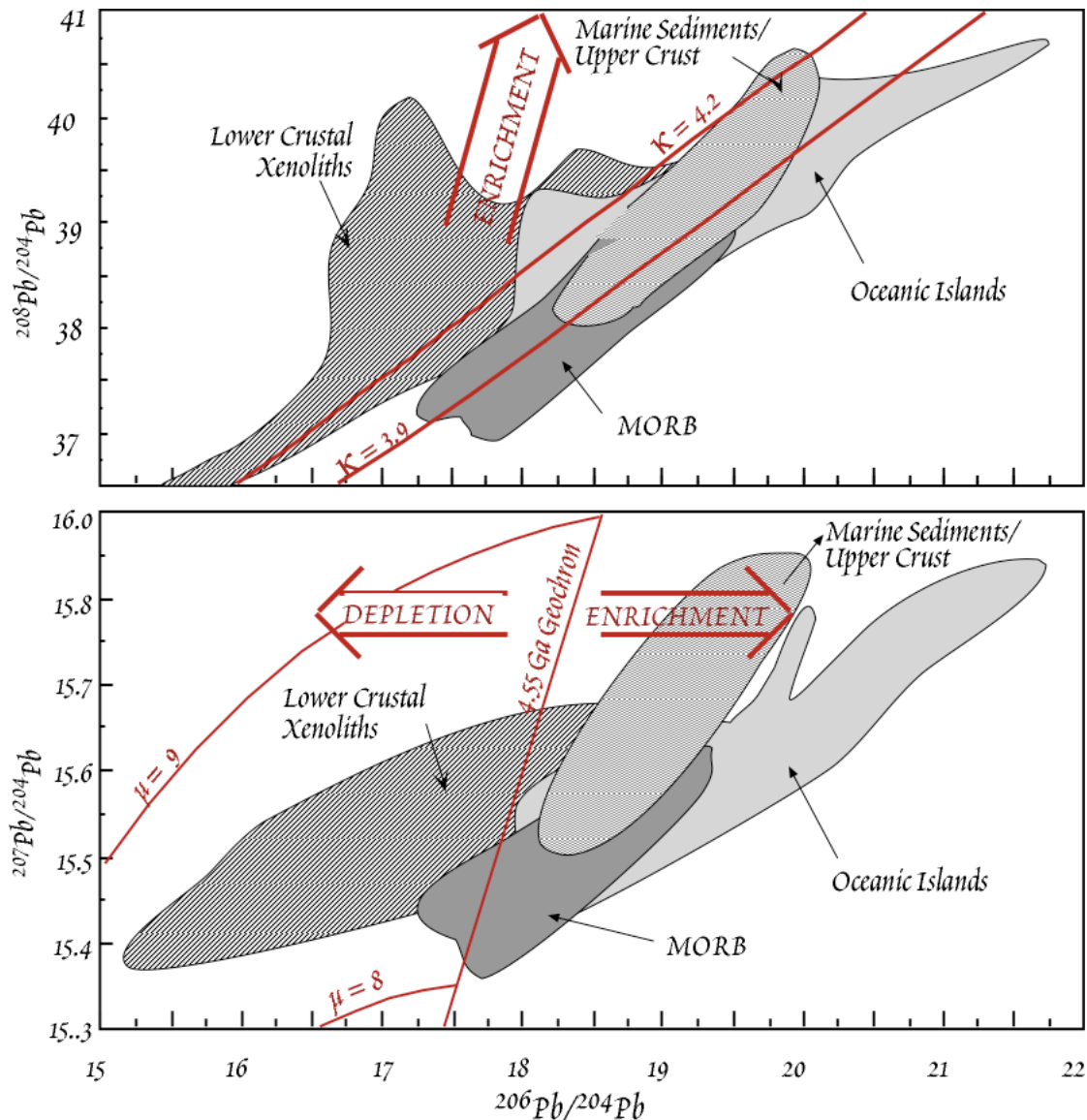
Figure 8.18. Pb isotope ratios in major terrestrial reservoirs. Typical lower continental crust and upper continental crust are represented by lower crustal xenoliths and modern marine sediments respectively (these somewhat underestimate the total variance in these reservoirs). MORB and oceanic islands represent the isotopic composition of upper mantle and deep mantle respectively.

If a system has experienced a decrease in U/Pb at some point in the past, its Pb isotopic composition will lie to the left of the Geochron; if its U/Pb ratio increased, its present Pb isotopic composition will lie to the right of the Geochron. U is more incompatible than Pb. This being the case, incompatible element depleted reservoirs should plot to the left of the Geochron, incompatible element enriched reservoirs should plot to the right of the Geochron (Figure 8.18). From the isotopic composition of other radiogenic elements, we would therefore predict that continental crust should lie to the right of the Geochron and the mantle to the left. Upper continental crustal rocks do plot mainly to the right of the Geochron, as expected, but surprisingly, Pb isotope ratios of mantle-derived rocks also plot mostly to the right of the Geochron (Figure 8.18). This indicates the U/Pb ratio in the mantle has increased, not decreased as expected. This phenomenon is known as the *Pb paradox* and it implies that a simple model of crust-mantle evolution that involves only transfer of incompatible elements from crust to mantle through magmatism is inadequate. We will discuss this in greater detail in Chapter 11.

The only large geochemical reservoir known to plot to the left of the Geochron is the lower continental crust. It is as yet unclear whether the four reservoirs represented on Figure 8.18, the upper crust, the lower crust, the upper mantle (as represented by MORB), and the deep mantle (as represented by oceanic islands) average to a composition that lies on the Geochron. If not, there must be some other reservoir within the Earth that has unradiogenic Pb (i.e., Pb falling to the left of the Geochron).

We can combine the growth equations for $^{208}Pb/^{204}Pb$ and $^{206}Pb/^{204}Pb$ in a way similar to equation 8.34. We end up with:

$$\frac{\Delta\ ^{208}Pb/\ ^{204}Pb}{\Delta\ ^{206}Pb/\ ^{204}Pb} = \frac{\kappa(e^{\lambda_{232}t} - 1)}{(e^{\lambda_{238}t} - 1)} \qquad 8.35$$

where, again, κ is the $^{232}Th/^{238}U$ ratio. Provided κ is constant in a series of cogenetic rocks (by cogenetic we mean that at t=0 they all had identical Pb isotope ratios), the slope of an array on a plot of $^{208}Pb/^{204}Pb$ and $^{206}Pb/^{204}Pb$ will depend only on t and κ, and not on the parent-daughter ratios. We can calculate κ from the slope of the data on a plot of $^{208}Pb/^{204}Pb$—$^{206}Pb/^{204}Pb$. U and Th are both highly incompatible elements. They have similar, but not identical, partition coefficients in most minerals. It seems unlikely that they will behave identically, and hence unlikely that κ will very often be constant. It can be shown that if κ varies and is positively correlated with variations in μ then equation 8.35, when solved for κ, will actually overestimate it.

8.4.7 U and Th Decay Series Isotopes

U and Th do not decay directly to Pb, rather the transition from U and Th to Pb passes through many intermediate radioactive daughters (Figure 8.19). Many of these daughters have very short half-lives, ranging from milliseconds to minutes, and are of little use to geochemists. However, a number of these intermediate daughters have half-lives ranging from days to hundreds of thousands of years and do provide useful information about geological processes. Table 8.4 lists half-lives and decay constants of some of the most useful of these nuclides.

The half-lives of all of these daughter isotopes are short enough so that any atoms present when the Earth formed have long since decayed (to Pb). They exist in the Earth (and in all other bodies of the solar system) only because they are continually produced by the decay of U and Th. The abundance of such an isotope depends on the balance between its own radioactive decay and its production by the decay of its parent:

$$\frac{dN_D}{dt} = \lambda_P N_P - \lambda_D N_D \qquad 8.36$$

Table 8.4. Half-lives and decay constants of long-lived U and Th daughters

Nuclide	Half-life, yrs	Decay constant, yr^{-1}	Parent
^{234}U	246,000	2.794×10^{-6}	^{238}U
^{231}Pa	32,480	2.134×10^{-5}	^{235}U
^{230}Th	75,200	9.217×10^{-6}	^{238}U
^{226}Ra	1,622	4.272×10^{-4}	^{238}U
^{228}Ra	6.7	1.06×10^{-1}	^{232}Th
^{210}Pb	22.26	3.11×10^{-2}	^{238}U

where subscripts P and D refer to parent and daughter respectively. This equation says simply that the rate of change of the abundance of the daughter isotope is equal to the rate of production less the rate of decay. This can be integrated to give:

$$N_D = \frac{\lambda_P}{\lambda_D - \lambda_P} N_P^0 \left(e^{-\lambda_p t} - e^{\lambda_D t}\right) + N_D^0 e^{-\lambda_D t} \qquad 8.37$$

Scientists dealing with the intermediate daughters of U and Th (and it is the daughters of ^{238}U that are of the most interest), generally work with activities, measured in the number of decays per unit time, rather than atomic abundances. One reason for this is that the abundances of these isotopes are generally determined by detecting their decay. Indeed, the shorter-lived ones are so rare they cannot be detected any other way. The other reason will become apparent shortly. Activities are related to atomic (molar) abundances by the basic equation of radioactive decay:
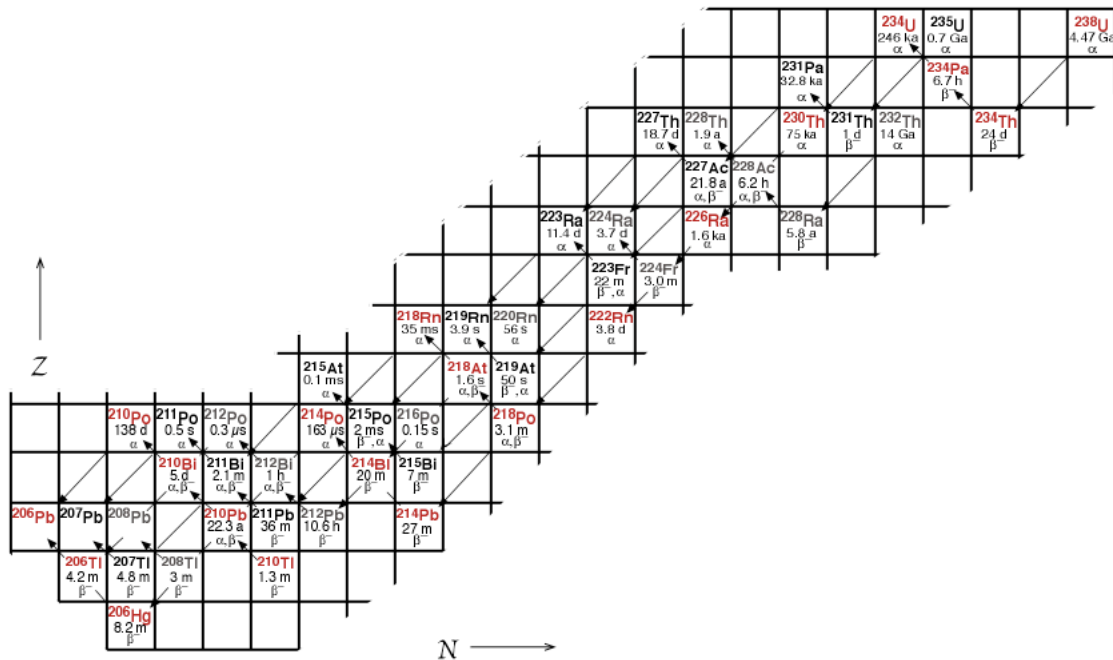
Figure 8.19. Part of the chart of the nuclides showing the series of decays that occur as ^{238}U, ^{235}U, and ^{232}Th are transformed to ^{206}Pb, ^{207}Pb, and ^{208}Pb respectively. Nuclides of the ^{238}U series are shown in red, the ^{232}Th series in gray, and the ^{235}U series in black.

$$\frac{dN_i}{dt} = -\lambda_i N_i \qquad\qquad 8.38$$

where dN_i/dt is the *activity* of i. Thus so long as we know the decay constant, we can calculate activity from concentration and visa versa. Activity is most commonly expressed in units of *disintegrations per minute* (dpm) per gram or per mole and is denoted by writing parentheses around the isotope (or the isotope ratio). Thus (^{234}U) is the activity of ^{234}U.

The state of *radioactive equilibrium* is the condition where their *activities* of the daughter and the parent are equal, i.e.:

$$\boxed{\frac{dN_D}{dt} = \frac{dN_P}{dt}} \qquad\qquad 8.39$$

It shares the same fundamental characteristic as the chemical equilibrium state: it is the state that will eventually be achieved if the system is not perturbed (remains closed). We can demonstrate this is so in two ways. The first is a simple mathematical demonstration. The equilibrium state is the steady state where the abundance of the daughter does not change, i.e., where the left hand side of 8.36 is zero:

$$0 = \lambda_P N_P - \lambda_D N_D \qquad\qquad 8.40$$

We substitute the dN/dt terms for the λN terms in 8.40, rearrange, and we obtain 8.39. QED.

The second demonstration is a thought experiment. Imagine a hopper, a grain hopper with an open top and a door in the bottom. The door is spring loaded such that the more weight placed on the door, the wider it opens. Suppose we start dropping marbles into the hopper at a constant rate. The weight of marbles accumulating in the hopper will force the door open slightly and marbles will start falling out at a slow rate. Because the marbles are falling out more slowly than they are falling in, the number and weight of marbles in the hopper will continue to increase. As a result, the door will continue to open. At some point, the door will be open so wide that marbles are falling out as fast as they are falling in. This is the steady state. Marbles can no longer accumulate in the hopper and hence the door is not forced to open any wider. The marbles falling into the door are like the decay of the parent isotope.

The marbles in the hopper represent the population of daughter isotopes. Their decay is represented by their passing through the bottom door. Just as the number of marbles passing through the door depends on the number of marbles in the hopper, the activity (number of decays per unit time) of an isotope depends on the number of atoms present.

If the rate of marbles dropping into the hopper decreases for some reason, marbles will fall out of the hopper faster than they fall in. The number of marbles in the hopper will decrease; as a result the weight on the door decreases and it starts to close. It continues to close (as the number of marbles decreases) until the rate at which marbles fall out equals the rate at which marbles fall in. At that point, there is no longer a change in the number of marbles in the hopper and the position of the door stabilizes. Again equilibrium has been achieved, this time with fewer marbles in the hopper, but nevertheless at the point where the rate of marbles going in equals the rate of marbles going out. The analogy to radioactive decay is exact.

Thus when a system is disturbed it will ultimately return to equilibrium. The rate at which it returns to equilibrium is determined by the decay constants of the parent and daughter. If we know how far out of equilibrium the system was when it was disturbed, we can determine the amount of time that has passed since it was disturbed by measuring the present rate of decay of the parent and daughter. Equilibrium is approached asymptotically, and these dating schemes are generally limited to time scales less than 5-10 times the half-life of the daughter. At longer times, the difference between actual activities and equilibrium ones becomes too small to measure reliably.

There are several useful dating methods based on the degree of disequilibria between U decay series nuclides. Our first example is ^{234}U-^{238}U dating of sediments. As may be seen from Figure 8.19, ^{234}U, which has a half-life of 246,000 years, is the 'great-granddaughter' of ^{238}U. For most purposes, the half-lives of the two intermediate daughters ^{234}Th and ^{234}Pa are so short that they can be ignored (because they quickly come into equilibrium with ^{238}U). As it turns out, ^{234}U and ^{238}U in seawater are not in equilibrium, i.e., the ^{234}U/^{238}U activity ratio is not 1. It is fairly constant, however, at about 1.15. The reason for this disequilibrium is that ^{234}U is preferentially leached from rocks because ^{234}U is present in rocks in damaged sites. It occupies the site of a ^{238}U atom that has undergone α-decay. The α particle and the recoil of the nucleus damage this site. Since it occupies a damaged site, it is more easily leached or dissolved from the crystal during weathering than ^{238}U. The oceans collect this 'leachate', hence they are enriched in ^{234}U. When U enters a sediment it is isolated from seawater (not necessarily immediately) and ^{234}U decays faster than it is created by decay of ^{238}U, so it slowly returns to the equilibrium condition where $(^{234}$U/^{238}U$) = 1$.

Let's now consider the problem from a mathematical perspective and derive an equation describing this return to equilibrium. We can divide the ^{234}U activity in a sample into that which is *supported* by ^{238}U, i.e., that amount in radioactive equilibrium with ^{238}U and that amount that is excess, i.e., *unsupported* by ^{238}U:

$$(^{234}U) = (^{234}U)_s + (^{234}U)_u \qquad\qquad 8.41$$

Subscripts *s* and *u* denote supported and unsupported. The activity of the excess ^{234}U decreases with time according to equation 8.4, which we can rewrite as:

$$(^{234}U)_U = (^{234}U)_U^0 e^{-\lambda_{234}t} \qquad\qquad 8.42$$

where the superscript naught denotes the initial unsupported activity (at $t = 0$). We can also write:

$$(^{234}U)_U^0 = (^{234}U)^0 - (^{234}U)_s \qquad\qquad 8.43$$

which just says that the initial unsupported activity of ^{234}U is equal to the total initial activity of ^{234}U less the (initial) supported activity of ^{234}U. *Since to a very good approximation the activity of the parent, ^{238}U, does not change over times on the order of the half-life of ^{234}U or even ten half-lives of ^{234}U, the present ^{238}U activity is equal to the activity at $t = 0$* (we make the usual assumption that the system is closed). By definition the supported activity of ^{234}U is equal to the activity of ^{238}U, both now and at t = 0, hence, 8.41 can be expressed as:

$$(^{234}U) = (^{238}U) + (^{234}U)_u \qquad\qquad 8.44$$

and 8.43 becomes $\qquad\qquad (^{234}U)_u^0 = (^{238}U) + (^{234}U)_u \qquad\qquad 8.45$

Substituting 8.45 into 8.42 yields:

$$\left({}^{234}U\right)_u = \left[\left({}^{234}U\right)^0 - \left({}^{238}U\right)\right]e^{-\lambda_{234}t} \qquad\qquad 8.46$$

Substituting 8.46 into 8.44, we have:

$$\left({}^{234}U\right) = \left({}^{238}U\right) + \left[\left({}^{234}U\right)^0 - \left({}^{238}U\right)\right]e^{-\lambda_{234}t} \qquad\qquad 8.47$$

Just as for other isotope systems, it is generally most convenient to deal with ratios rather than absolute activities (among other things, this allows us to ignore detector efficiency provided the detector is equally efficient at all energies of interest), hence we divide by the activity of ^{238}U:

$$\left(\frac{{}^{234}U}{{}^{238}U}\right) = 1 + \left[\frac{\left({}^{234}U\right)^0 - \left({}^{238}U\right)}{\left({}^{238}U\right)}\right]e^{-\lambda_{234}t} \qquad\qquad 8.48$$

or since $^{238}U = {}^{238}U°$:

$$\left(\frac{{}^{234}U}{{}^{238}U}\right) = 1 + \left[\left(\frac{{}^{234}U}{{}^{238}U}\right)^0 - 1\right]e^{-\lambda_{234}t} \qquad\qquad 8.49$$

Corals, for example, concentrate U. If we measure the $({}^{234}U/{}^{238}U)$ ratio of an ancient coral, and can assume that the seawater in which that coral grew had a $({}^{234}U/{}^{238}U)$ the same as modern seawater (1.15), then the age of the coral can be obtained by solving equation 8.49 for t.

Because the disequilibrium between ^{230}Th and ^{238}U can be much larger than between ^{234}U and ^{238}U, ^{230}Th-^{238}U disequilibria is a more commonly used dating scheme than is ^{234}U-^{238}U. ^{230}Th is the daughter of ^{234}U (the decay chain is $^{238}U \rightarrow {}^{234}Th + \alpha$, $^{234}Th \rightarrow {}^{234}Pa + \beta^-$, $^{234}Pa \rightarrow {}^{234}U + \beta^-$, $^{234}U \rightarrow {}^{230}Th + \alpha$). To simplify the math involved, let's assume ^{234}U and ^{238}U are in radioactive equilibrium. In high temperature systems, this is a very good assumption because α–damaged sites, which cause the disequilibrium noted above, are quickly annealed. With this assumption, we can treat the production of ^{230}Th as if it were the direct decay product of ^{238}U. We write an equation analogous to 8.41 and from it derive an equation analogous to 8.47:

$$\left({}^{230}Th\right) = \left({}^{238}U\right) + \left[\left({}^{230}Th\right)^0 - \left({}^{238}U\right)\right]e^{-\lambda_{230}t} \qquad\qquad 8.50$$

We divide by the activity of ^{232}Th:

$$\left(\frac{{}^{230}Th}{{}^{232}Th}\right) = \left(\frac{{}^{238}U}{{}^{232}Th}\right) + \left[\left(\frac{{}^{230}Th}{{}^{232}Th}\right)^0 - \left(\frac{{}^{238}U}{{}^{232}Th}\right)\right]e^{-\lambda_{230}t} \qquad\qquad 8.51$$

and rearranging:

$$\left(\frac{{}^{230}Th}{{}^{232}Th}\right) = \left(\frac{{}^{230}Th}{{}^{232}Th}\right)^0 e^{-\lambda_{230}t} + \left(\frac{{}^{238}U}{{}^{232}Th}\right)(1 - e^{-\lambda_{230}t}) \qquad\qquad 8.52$$

$^{230}Th/{}^{238}U$ is commonly used to date sediments and to determine sedimentation rates. However, unlike the case of $({}^{234}U/{}^{238}U)°$, $({}^{230}Th/{}^{232}Th)°$ is not *a priori* known, so there are 2 unknowns in equation 8.52. As was the case for isochrons, however, we can solve for these 2 unknowns if we have a series of two or more measurements on sediments with the same initial $({}^{230}Th/{}^{232}Th)$. Example 8.5 demonstrates how this is done for the case of a Mn nodule. In other cases, corals, for example, we can assume that $({}^{230}Th/{}^{232}Th)°$ is the same as in modern seawater.

Th–U disequilibria may also be used for dating lavas, and we now turn our attention briefly to this application. Equation 8.52 has the form of a straight line on a $({}^{230}Th/{}^{232}Th)$ — $({}^{238}U/{}^{232}Th)$ plot; the first term is the intercept and $(1 - e^{-\lambda_{230}t})$ is the slope. Since the slope is proportional to time, a line on a $({}^{230}Th/{}^{232}Th)$ — $({}^{238}U/{}^{232}Th)$ plot is an isochron, though unlike a conventional isochron the intercept also changes with time (Figure 8.21).

To understand how this works, imagine a crystallizing magma with homogeneous $({}^{230}Th/{}^{232}Th)$ and $({}^{238}U/{}^{232}Th)$ ratios. Th and U partition into different minerals differently, so the minerals will have variable $({}^{238}U/{}^{232}Th)$ ratios but constant $({}^{230}Th/{}^{232}Th)$ ratios (assuming crystallization occurs quickly

EXAMPLE 8.5. DETERMINING THE GROWTH RATE OF A Mn NODULE

The tops of manganese nodules grow by precipitation of Mn-Fe oxides and hydroxides from seawater. They are known to grow very slowly, but how slowly? If we assume the rate of growth is constant then depth in the nodule should be proportional to time. If z is the depth in the nodule, and s is the growth (sedimentation) rate, then:

$$t = z/s \qquad\qquad 8.53$$

and 8.52 becomes:
$$\left(\frac{^{230}Th}{^{232}Th}\right) = \left(\frac{^{230}Th}{^{232}Th}\right)^0 e^{-\lambda_{230}z/s} + \left(\frac{^{238}U}{^{232}Th}\right)(1 - e^{-\lambda_{230}z/s}) \qquad 8.54$$

At the surface of the nodule, $z = 0$, so the exponential terms both go to 1 and the measured activity ratio is initial activity ratio. Having a value for $(^{230}Th/^{232}Th)^\circ$, equ. 8.54 can then be solved for s, the growth rate if measurements are made at some other depth.

In practice, however, it is difficult to obtain a sample exactly at the surface: a finite amount of material is required for analysis, and this often tr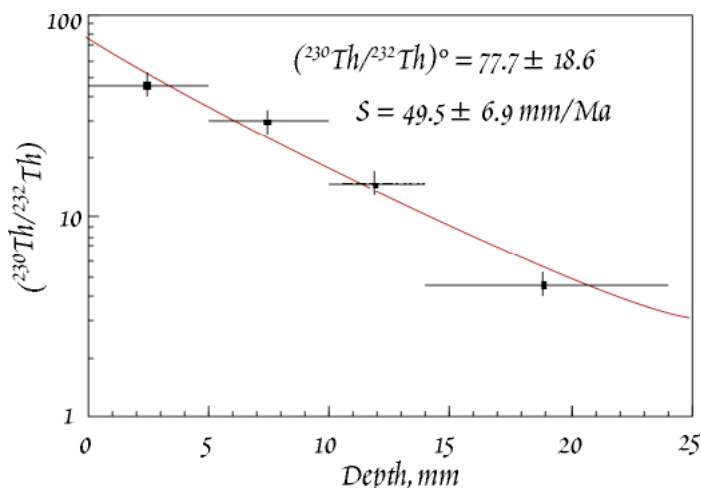anslates into a layer of several mm thickness. Equation 8.54 is solved in that instance by less direct means. For example, consider the data shown in Figure 8.20 on a Pacific manganese nodule reported by Huh and Ku (1984). In this plot of $(^{230}Th/^{232}Th)$ vs. depth, the initial ratio is the intercept of the best-fit line through the data. A growth rate was obtained by obtaining an initial guess of the initial $(^{230}Th/^{232}Th)$, then iteratively refining the solution to 8.54 by minimizing the difference between computed and observed activity ratios. A growth rate of 49.5 mm/Ma and a $(^{230}Th/^{232}Th)$ of 77.7 was found to best fit the observations.

$(^{230}Th/^{232}Th)^\circ = 77.7 \pm 18.6$

$S = 49.5 \pm 6.9\ mm/Ma$

Figure 8.20. $(^{230}Th/^{232}Th)$ as a function in depth in a manganese nodule from MANOP Site H. After Huh and Ku (1984).

compared to the half-life of Th) since these two isotopes are chemically identical. Thus the minerals will plot on a horizontal line in Figure 8.21 at $t = 0$. After the system closes, ^{238}U and ^{230}Th will begin to come to radioactive equilibrium (either ^{230}Th will decay faster than it is produced or visa versa, depending on whether $(^{230}Th/^{238}U)$ is greater than or less than 1, the equilibrium value). Thus the original horizontal line will rotate, as in a conventional isochron diagram, but unlike the conventional isochron diagram, the intercept also changes. The rotation occurs about the point where $(^{230}Th/^{232}Th) = (^{238}U/^{232}Th)$, which is known as the *equipoint*. As t approaches infinity, the exponential term approaches 1 and:

$$\lim_{t\to\infty}\left(\frac{^{230}Th}{^{232}Th}\right) = \left(\frac{^{238}U}{^{232}Th}\right) \qquad\qquad 8.55$$

Thus the equilibrium situation, the situation at $t=\infty$, is $(^{230}Th/^{232}Th) = (^{238}U/^{232}Th)$. In this case, all the minerals will fall on a line, having a slope of 1. This line is known as the *equiline*.

^{226}Ra is another relatively long-lived nuclide ($t_{1/2} = 1600$ yr) that has proved useful in dating igneous rocks. The fundamentals are precisely analogous to those we have discussed for ^{234}U and ^{230}Th, with one exception. Unfortunately, Ra has no stable isotope to which one can ratio ^{226}Ra. Therefore, the assumption is made that Ra behaves as Ba, and the abundance of Ba is used to form a ratio.

Figure 8.22 shows ^{230}Th–^{238}U and ^{226}Ra–^{230}Th isochrons obtained on mineral separates, groundmass, and a whole rock sample from the Castle Creek andesite of Mt. St. Helens. Conventional dating tech-
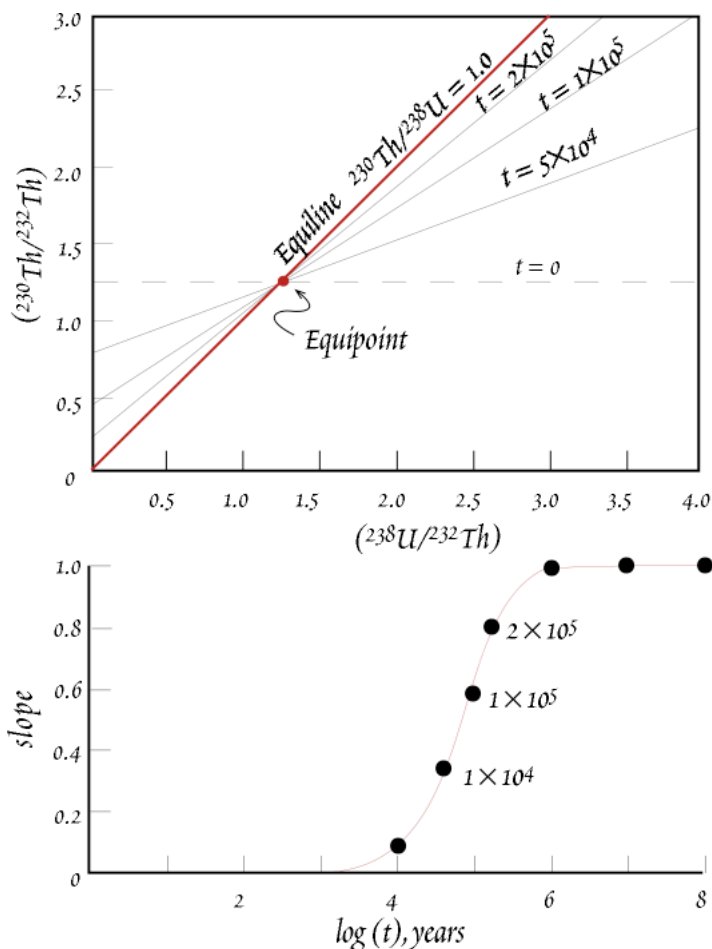
niques indicate this lava is only about 2000 years old, but both the ^{230}Th–^{238}U and ^{226}Ra–^{230}Th give much older ages. The ^{230}Th/^{232}Th–^{238}U/^{232}Th data define a 27±12 ka isochron. This suggests the crystals in the magma may have crystallized as much as 20,000 years or more before eruption. The age ^{226}Ra–^{230}Th is less precise because the slope is only slightly less than 1, and all samples seem to contain excess ^{226}Ra. Nevertheless, the slope of the data is clearly greater than that of a 2 ka isochron, so these data also suggest the crystallization significantly predated eruption. According to Volpe and Hammond (1991) the difference in the ^{230}Th–^{238}U and ^{226}Ra–^{230}Th ages may reflect changes in melt composition, perhaps due to assimilation of country rock or addition of a Ra-rich gas or fluid phase to the magma. ^{230}Th–^{238}U and ^{226}Ra–^{230}Th ages of the more recent eruptive products of Mt. St. Helens, including the 1980-1986 eruptive phase, were closer to the eruption ages. For example, Volpe and Hammond (1991) obtained a ^{230}Th–^{238}U age of 6±4 ka on the 1982 dacite. Volpe and Hammond (1991) suggested that there was a significant volume of older magma still present in the magma chamber when the most recent eruptive stage of Mt. St. Helens began about 4000 years ago, and that this older magma has been progressively replaced by fresh magma over the past 4000 years.

Figure 8.21. (a) ^{230}Th—^{238}U isochron diagram. The (^{238}U/^{232}Th) of the source is given by the intersection of the isochron with the equiline. (b) shows how the slope changes as a function of time. After Faure (1986).

There are also important geochemical, as opposed to geochronological, inferences that can be made from ratios of (^{230}Th/^{232}Th) and (^{238}U/^{232}Th) in zero-age igneous rocks. The degree of disequilibrium between ^{230}Th and ^{238}U in such rocks depends on the extent of fractionation between Th and U during melting and the rate at which melting occurs. This in turn depends on the mineralogy in the mantle undergoing melting, the extent of melting, rates of melt percolation, and other factors. Thus some interesting inferences about melting in the mantle can be made from these isotope ratios. We will discuss these in subsequent chapters.

In the past, the activities of U-decay series isotopes were measured by alpha-counting and fairly large quantities of material are necessary. Improvements in mass spectrometry made it possible to measure ^{234}U, ^{230}Th, and other key nuclides such as ^{231}Pa and ^{226}Ra on smaller quantities of material and with much better precision than α counting. This has led to a considerable expansion of applications of U-decay series isotopes.

8.4.8 ISOTOPES OF HE AND OTHER RARE GASES

Helium

Alpha particles are, of course, simply ^{4}He nuclei, and therefore ^{4}He is produced by alpha decay of U and Th. Thus the ratio of ^{4}He/^{3}He varies in the Earth. Unlike virtually all other elements, He is not conserved on the Earth: much of the He present when the Earth formed has been subsequently lost. Be-

ing a rare gas, He does not combine chemically with anything, and it also diffuses rapidly (Ever had a He balloon? How long did it last?) Helium brought to the Earth's surface by magmatism eventually finds its way into the atmosphere. Once there, it can escape from the top of atmosphere because of its low mass*. (H^2 also escapes from the atmosphere, but most H is bound up as water or hydrous minerals, so relatively little is lost.) Since ^4He is continually produced and, for all practical purposes, ^3He is not, it should not be surprising that the $^4He/^3He$ ratio in the Earth is a very large number. For some reason, perhaps because geochemists like to deal with very small numbers rather than very large ones, or perhaps because it actually ^3He that is most interesting, the He isotope ratio is generally expressed as $^3He/^4He$, in contradiction to the normal convention of placing the radiogenic isotope in the numerator. We will adhere to this particular convention of not adhering to the convention and use the $^3He/^4He$ ratio.

The $^3He/^4He$ ratio of the atmosphere is 1.384 x 10^{-6}. Since this ratio is uniform and atmospheric He available to all laboratories, it is a convenient standard and moreover provides the basis for a convenient normalization. He ratios are often reported and discussed relative to the atmospheric value. The units are called simply R/R_A, where R_A indicates the atmospheric ratio.

Actually, it is not quite true that ^3He is not produced in the Earth. It is produced in very small quantities through the nuclear reaction: $^6Li(n,\alpha)\rightarrow^3H(\beta)\rightarrow^3He$, which is to say ^6Li is excited by the capture of a neutron that has been produced by U fission, and decays through the emission of an alpha particle to tritium, which beta decays to ^3He. As a result He in crustal rocks has an $R/R_A \approx 0.1 - 0.01$ (the exact ratio varies with the Li/U ratio). ^3He can also be produced in the atmosphere and surface of the Earth by cosmic ray spallation reactions. Up to about 25 years ago, all He was thought to be a product of these processes (radiogenic and cosmogenic). Then helium with R/R_A around 1.22 was discovered in Pacific deep water in 1969 (Clark et al., 1969). Subsequently, Lupton and Craig (1975) discovered that mid-ocean ridge basalt glasses had high $^3He/^4He$ ratios. The gases are trapped in the glassy rims of basalts by the combined effects of hydrostatic pressure and rapid quenching. Measurements in 1974 and 1975 found such basalts had $R/R_A \approx 9$. It was clear that a 'primordial' He component was trapped in the Earth's interior and is constantly escaping. Subsequent measurements have shown that the $^3He/^4He$ of MORB is quite uniform around $R/R_A \approx 8.5\pm1$. This is only primordial in a relative sense: gas-rich meteorites have an $R/R_A \approx 200$. Thus even in MORB, He is 95% radiogenic.
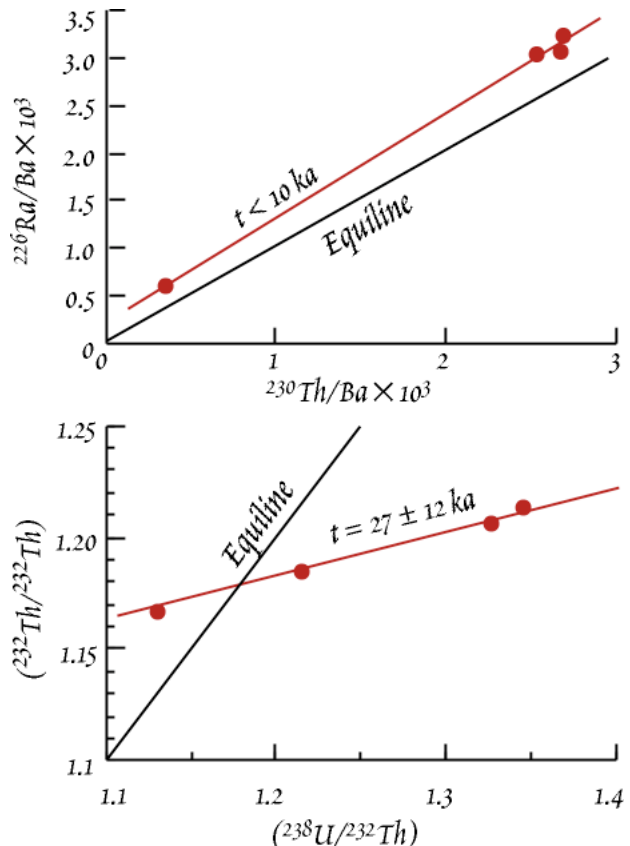

Figure 8.22. ^{230}Th–^{238}U and ^{226}Ra–^{230}Th mineral isochrons for the Castle Creek andesite of Mt. St. Helens. ^{14}C and tree ring chronology indicate this lava was erupted 1700-2200 years ago. After Volpe and Hammond (1991).

---

*At equilibrium the average kinetic energy of all variety of molecules in a gas will be equal. Since kinetic energy is related to velocity by $E=^1/_2mv^2$, and since the mass of He is lower than for other species, the velocities of He atoms will be higher and more likely to exceed the escape velocity. In actuality, however, escape of He is more complex than simple thermal acceleration and involves other processes such as acceleration of He ions by the Earth's magnetic field.
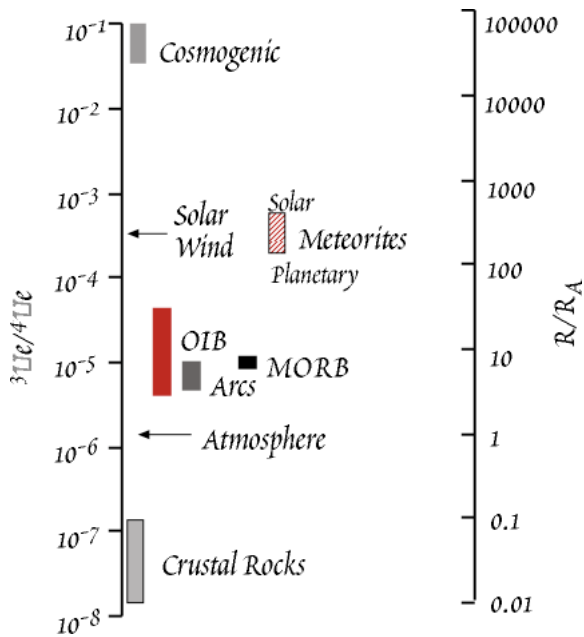
Figure 8.23. He isotope ratios in various terrestrial and solar system materials. "Solar" and "Planetary" refer to the solar and planetary components in meteorites. "Crustal rocks" shows the values expected for *in situ* production from α decay and neutron-induced nuclear reactions.

Figure 8.23 illustrates the He isotopic composition of various terrestrial reservoirs. Oceanic islands and other hotspots often have even higher ratios, up to about $R/R_A \approx 40$, though some islands, Tristan da Cunha for example, have lower ratios: $R/R_A \approx 5$ (e.g., Kurz et al., 1982). This suggests that most oceanic island basalts are derived from a less degassed, and in that sense more primordial, reservoir than MORB. This is consistent with the mantle plume hypothesis.

Island arc volcanics (IAV) seem also to be fairly uniform with $R/R_A \approx 6$ (Lupton, 1983). Ratios lower than MORB suggest the presence of a slab-derived component, but also indicate most of the He in IAV comes from the mantle wedge (a conclusion similar to the one reached from other radiogenic isotopes).

Two interesting developments are the discovery of cosmogenic He in Hawaiian basalts (Kurz, 1987), and very high R/R_A in some very slowly accumulating marine sediments. The former is a result of the $^6Li(n,\alpha) \rightarrow {}^3H(\beta) \rightarrow {}^3He$ reaction instigated by cosmic-ray produced neutrons and spallation*. The cosmogenic component decreases rapidly with depth of the rock (it is largely restricted to the top meter) and increases with elevation above sealevel (the effect was noticed at the summit of Haleakala at 2000m). Thus one should be suspicious of high $^3He/^4He$ ratios in old (100,000 yrs or more) subareal

rocks. R/R_A as high as 226 (and as low as 0.03) have also been observed in diamonds. The meaning of this was not immediately clear, but the origin of these diamonds is unknown, and the most probable explanation is that the diamonds were mined from a placer and that the He is cosmogenic. Very high

R/R_A in some very slowly accumulating marine sediments is probably an effect of accumulation of cosmic dust in sediment. $^{40}Ar/^{36}Ar$ ratios lower than atmospheric have also been observed in deep-sea sediment. A final development was the realization that He ratios of magma could change, through the combined effect of diffusion out of the magma and radiogenic growth of He, on the time scale of residence time of magma in a magma chamber (Zindler and Hart, 1986). This means we must be cautious of low $^3He/^4He$ ratios as well.
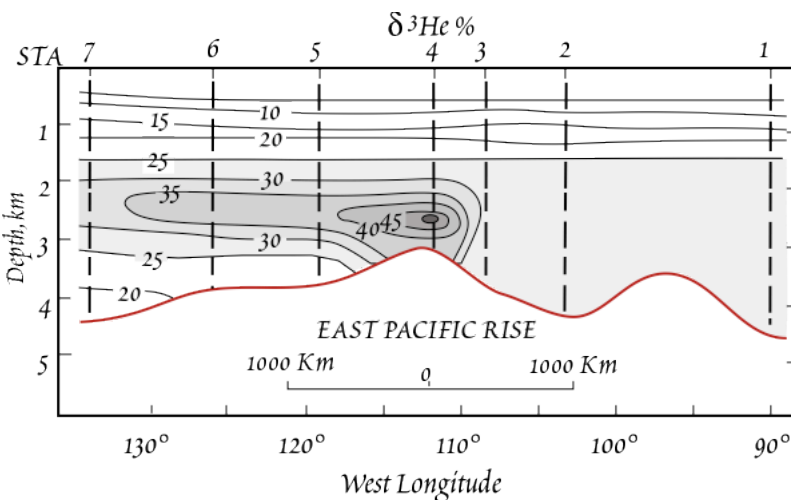

Figure 8.24. Contours of relative ^3He concentrations in seawater over the East Pacific Rise (Lupton and Craig, 1981).

---

* Spallation is the process in which a necleus breaks into smaller nucleii as a result of a collision with a very high energy particle such as a cosmic ray.

Since He is injected at mid-ocean ridges, particularly in the Pacific, at depths of 2500-3000 meters, He isotopes can be used to trace water mass movements. Figure 8.24 shows the He plume of hydrothermal activity on the East Pacific Rise. Interestingly, the plume indicates water is flowing in the direction opposite to that which the physical oceanographers had thought. Another application is prospecting for ridge-crest hydrothermal activity. Several hydrothermal areas (including the first one) have been discovered from the He isotope anomalies in the water column. ^{4}He is also used as a tracer in U prospecting.

8.4.8.1 NEON

Neon has perhaps the most puzzling isotopic systematics of the noble gases. Ne has three isotopes, ^{20}Ne, ^{21}Ne, and ^{22}Ne. Though none of them are radiogenic, the isotopic composition of neon varies in the Earth as well as extraterrestrial materials (Figure 8.25). Two processes have apparently produced these isotopic variations: mass-dependent fractionation (which we cover in the next chapter) and nuclear reactions such as $^{18}O(\alpha,n) \rightarrow {}^{21}$Ne, $^{24}Mg(n,\alpha) \rightarrow {}^{21}$Ne, and $^{25}Mg(n,\alpha) \rightarrow {}^{22}$Ne, with the α particles and neutrons coming from α decay and fission respectively. Production rates are quite small, for example about 4.2×10^{-22} cc/g of ^{21}Ne in the mantle. The production rate of ^{21}Ne is about an order of magnitude higher than that of ^{20}Ne and ^{22}Ne, and ^{21}Ne is the least abundant of the Ne isotopes (0.27%), so the effect of these reactions is to increase the ^{21}Ne/^{22}Ne ratio without changing the ^{20}Ne/^{22}Ne ratio. In addition, nucleosynthetic processes are apparently responsible for some of the Ne isotopic variations in meteorites (see Chapter 10).

Noble gases trapped in basalts from mid-ocean ridges and basalts and mantle xenoliths from oceanic islands form arrays that diverge from atmospheric composition to compositions with higher ^{20}Ne/^{22}Ne and ^{21}Ne/^{22}Ne (e.g., Sarda, et al., 1988; Poreda and Farley, 1992). Accroding to Farley and Poreda (1993), the array reflect contamination of mantle Ne by atmospheric Ne; in essence, they are mixing arrays between mantle components with high ^{20}Ne/^{22}Ne and variable ^{21}Ne/^{22}Ne ratios. The very low concentrations of He in the atmosphere minimizes the problem of contamination in basalts; but atmospheric concentrations of the heavier noble gases, including Ne, are higher, so this is much more of a problem in the case of these gases.

Even though the arrays themselves are the products of contamination, the variation in the slope of the arrays is significant and indicates variation of ^{21}Ne/^{22}Ne in the mantle, with the MORB source having higher ^{21}Ne/^{22}Ne and OIB sources. This would be consistent with the MORB source being more degassed and hence having lower Ne concentrations. Addition of nuclogenic Ne would have a larger effect on ^{21}Ne/^{22}Ne in that case.

Two hypotheses have been proposed to explain the observed isotopic variations in the Earth. In
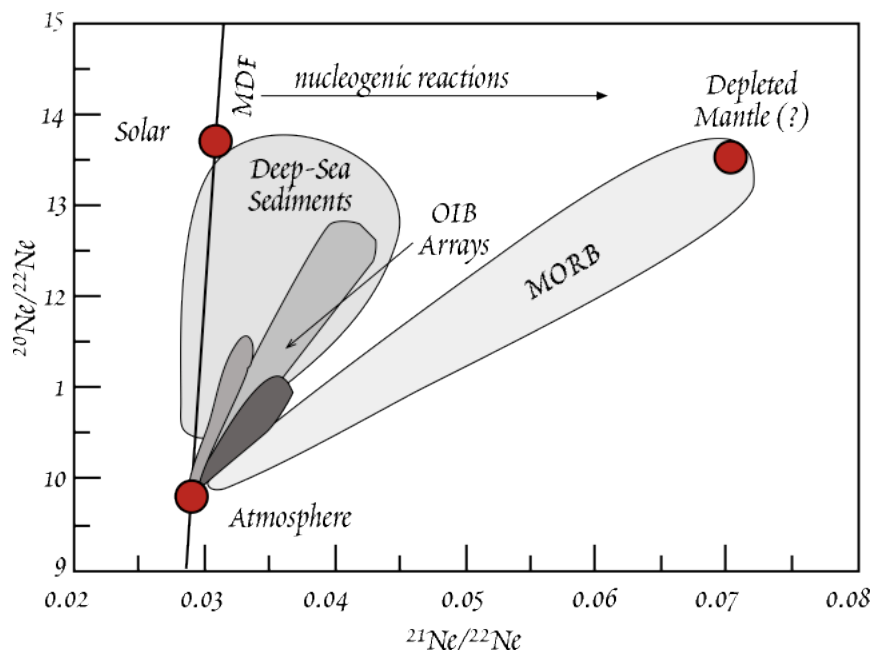
Figure 8.25. Ne isotope ratios in terrestrial materials. The line marked "MDF" is the mass dependent fractionation line. The line has a slope of 2 because the change in ^{20}Ne/^{22}Ne resulting from fractionation should be twice that of ^{21}Ne/^{22}Ne because the mass difference between ^{20}Ne and ^{22}Ne is twice that between ^{21}Ne and ^{22}Ne. OIB arrays are data fields for basalts and mantle xenoliths from Samoa and Hawaii.

the model advocated by Japanese workers (e.g., Honda et al., 1991; Ozima and Zahnle, 1993), the Earth initially formed with an Ne isotopic composition similar to that of solar wind. During the Earth's very early history, much of Earth's atmophile element inventory escaped from the interior, perhaps during the existence of a magma ocean, to form a hot, massive atmosphere. Much of the hydrogen and helium and a significant fraction of the neon escaped the atmosphere during this time. The efficiency of escape will depend on the mass of the molecule, so that the proportional loss of ^{20}Ne is greatest and that of ^{22}Ne the least. Thus the isotopic composition of the residual atmosphere has lower ^{20}Ne/^{22}Ne and ^{21}Ne/^{22}Ne than the original one.

Subsequently, the ^{21}Ne/^{22}Ne in the degassed mantle increased due to nucleogenic production of ^{21}Ne. Portions of the mantle that experienced greater degassing should have higher ^{21}Ne/^{22}Ne than less degassed portions. Thus MORB apparently sample the most degassed mantle, presumably the upper mantle, while oceanic island basalts and xenoliths are apparently derived from a less degassed part of the mantle, presumably mantle plumes originating in the deep mantle.

Allègre et al. (1993) proposed a somewhat different model, one inspired by the observation that slowly accumulating pelagic sediments have Ne isotope ratios different from atmospheric, apparently due to the presence of cosmic dust and micrometeorites in the sediment. They suggest that the Earth original formed with a Ne isotopic composition similar to the present mantle. According to them, subduction of deep sea sediments has increased the ^{20}Ne/^{22}Ne ratio of the degassed mantle. Nucleogenic production in the mantle then increases the ^{21}Ne/^{22}Ne ratio, and this effect has been greatest in the most degassed portion of the mantle, which is presumably sampled by MORB.

8.4.8.2 K-Ar-Ca

There are several aspects of the K-Ar system that make it particularly advantageous for some geochronological applications. First ^{40}K has one of the shortest half-lives of the decay systems in Table 8.2, making it more useful for dating young rocks than the other systems. In favorable cases, K-Ar ages on rocks as young as 30,000 yrs can be obtained with useful precision. Second, Ar is a rare gas and in most lavas it is virtually totally lost upon eruption. With no initial component, an age can be obtained from a single K-Ar determination. Being a rare gas, Ar diffuses somewhat more readily than other elements. Further, K is concentrated in sheet silicates such as micas, which have comparatively open crystal structures. As a result, the closure temperature for the K-Ar system is low, making it a useful system for study of relatively low temperature phenomena (such as petroleum genesis). This of course, can be a disadvantage, as it means the K-Ar system is reset rather easily.

From a geochemical viewpoint, the K-Ar system is of most interest with respect to the degassing of the Earthand evolution of the Earth's atmosphere. The most important questions in this regard are: what proportion of the Earth has been degassed, how extreme has this outgassing been, and when did this degassing occur? To briefly illustrate how K-Ar systematics can address these problems, consider the second question. We can think of two extreme possibilities: outgassing occurred yesterday; outgassing occurred simultaneously with the formation of the Earth. If outgassing occurred yesterday, then the ^{40}Ar/^{36}Ar ratio of the Earth's interior will be the same as that of the atmosphere. If outgassing occurred early in Earth's history then the ^{40}Ar/^{36}Ar ratio of the atmosphere should be close to the initial ratio for the solar system and the ^{40}Ar/^{36}Ar of the Earth's interior should be much higher because of the decay of ^{40}K over the history of the Earth. In actuality, neither of these models match observation. The ^{40}Ar/^{36}Ar ratio measured in MORB, in which noble gases are trapped by the pressure prevailing on the ocean floor, is very much higher than in the atmosphere. Ratios in MORB can be as high as 40,000, whereas that of the atmosphere is uniform at 295.5. So the Earth did not outgas yesterday. On the other hand, the atmospheric ratio is much higher than the solar system initial ratio. Indeed, the solar system initial ratio is less than 1, so most of the Ar in the atmosphere is actually radiogenic. Consequently, we can conclude that substantial degassing occurred after the Earth formed.

Now let's consider the first question: how much of the Earth has degassed. As we mentioned essentially all the Ar in the atmosphere is radiogenic. Since both the concentration of Ar and its isotopic composition are uniform in the atmosphere, it is fairly easy to estimate the amount of ^{40}Ar in the atmosphere, which works out to be 1.65 x 10^{18} moles. The K concentration is the silicate part of the Earth is about 250±50 ppm, which corresponds to 2.56±0.5 x 10^{22} moles of K. Over the 4.56 Ga of Earth's his-

tory, this amount of K should have produced about $3.5\pm0.7 \times 10^{18}$ moles of Ar. Thus about half ($\pm10\%$) of the Ar that we expect has been produced by radioactive decay in now in the atmosphere; the remainder must still be in the solid Earth. It is fairly easy to show that most of this must be in the mantle rather than the crust (Allegre et al., 1996).

Combining Ar systematics with isotope systematics of other noble gases, there seems to be consensus on these points: (1) the Earth probably lost its early, primitive atmosphere, (2) the present atmosphere is a product of degassing of the Earth's interior, (3)

Table 8.5. Some Cosmogenic Nuclides of Geologic Interest

Nuclide	Half-life (y)	λ (y^{-1})
^{10}Be	1.5×10^6	0.462×10^{-6}
^{14}C	5730	0.1209×10^{-3}
^{26}Al	0.716×10^6	0.968×10^{-6}
^{36}Cl	0.308×10^6	2.25×10^{-6}
^{39}Ar	269	0.257×10^{-2}

much, perhaps half or more, of the mantle has been degassed rather extensively, and (4) most of the degassing occurred in Earth's history, probably shortly after it formed. Beyond these points, there is considerable disagreement.

Most of ^{40}K (90%) decays to ^{40}Ca. But this decay scheme has not yielded much geochemical or geochronological information thus far. The reason is the low ratio of ^{40}K to ^{40}Ca in most geological materials, which in turn means the radiogenic contribution to ^{40}Ca is small and ^{40}Ca/^{42}Ca variations are very small. Also since the isotopes are rather light, they are comparatively easily fractionated. Indeed, it has been shown that they can be fractionated by the chemical techniques used to separate Ca. The variation of ^{40}Ca/^{42}Ca is so small that in one good geochronological age determination, the initial ^{40}Ca/^{42}Ca ratio of the Pike's Peak batholith (age 1 Ga) was found to be indistinguishable from the initial ratio in meteorites. Work by Marshall and DePaolo (1987) showed that MORB have ε_{Ca} values (ε_{Ca} is defined in exactly the same sense and ε_{Nd} and ε_{Hf}) around 0. Thus although the source of mid-ocean ridge basalts has been depleted in K relative to Ca, this has not produced Ca isotope ratios significantly different from that of the bulk Earth. As a result of high K/Ca ratios, crustal rocks have slightly positive ε_{Ca} ratios. Interestingly, a number of island arc volcanics have ε_{Ca} in the range of 1-2, which is consistent with the hypothesis that their source contains a crustal component, a hypothesis based on the isotopic compositions of Pb, Sr and Nd in them.

8.5 Cosmogenic and Fossil Isotopes

The Earth is constantly bombarded by 'cosmic rays' (we shouldn't feel picked on, the entire cosmos is). These are atomic nuclei (mostly H) stripped of their electrons and traveling at relativistic velocities. Some originate in the Sun, but most originate in high-energy regions of the cosmos such as supernovae. For the most part their origin is not well understood. What is understood is that they have sufficient energy to shatter a nucleus when they collide with one. The nucleus breaks into several parts in a process called *spallation*.

Having mass and charge, cosmic rays don't have much penetrating power. Thus the intensity of cosmic radiation increases with increasing altitude in the atmosphere (indeed, this is how they were shown to be of cosmic origin). Most are stopped in the atmosphere, their interactions creating a cascade of lesser energy particles, or are slowed considerably. Even if they don't score a direct hit, they lose energy through electromagnetic interaction with matter (ionizing the atoms they pass by). Thus cosmic rays have their greatest effect in the atmosphere and somewhat less of an effect in the uppermost few centimeters or so of rock.

The nuclear effects of cosmic radiation are on the whole pretty trivial. Nitrogen and oxygen, being the principal constituents of the atmosphere are the most common targets, yet their is no change in the isotopic abundances of these elements. Cosmic radiation is most interesting because of the production of nuclides whose half-lives are so short they would not otherwise exist. The nuclides of greatest interest are listed in Table 8.5 along with their half-lives and their decay constants. These nuclides are created either directly through spallation (e.g., ^{10}Be), or by nuclear reactions with particles produced by spallation, e.g., ^{14}C: ^{14}N (n,p)$\rightarrow^{14}$C. We have space only to briefly consider a few of the many applications of cosmogenic nuclides.

8.5.1 ^{14}C

The best known of the cosmogenic nuclide dating methods is ^{14}C, of course. It is useful in dating archaeological, climatological, volcanological, seismological, paleontological, etc., 'events'. Present technology utilizes accelerator mass spectrometry rather than traditional β-counting and useful information on samples as old as 40,000 years can be produced. The principle of this method is quite simple. One assumes a constant production of ^{14}C in the atmosphere. The atmosphere is well mixed and has a uniform ^{14}C/^{12}C ratio. The isotope ratio of carbon isolated from the atmosphere by plants will decrease with time according to:

$$\frac{^{14}C}{^{12}C} = \left(\frac{^{14}C}{^{12}C}\right)_0 e^{-\lambda_{14}t}$$

8.56

If the production rate is constant, the 'naught' value is the present day atmospheric value. In practice, ^{14}C is generally reported in unites of activity of ^{14}C per gram carbon – which is defined as the *specific activity.*

Research over the last 50 years has demonstrated that the production rate of ^{14}C has certainly not been constant; and it can be inferred from this that the cosmic ray flux has not been constant. The primary cause of this variation is variation in solar activity and the amount of solar wind. Solar wind consists of charged particles and the electromagnetic field associated it with deflects some fraction of cosmic rays that would otherwise enter the solar system and strike the Earth. In addition to this, the ^{14}C/^{12}C ratio in the present atmosphere is somewhat lower than it has been in the recent past due to dilution with CO_2 released by extensive burning of fossil fuels.

To get around the problem of the non-constant production rate, ^{14}C ages have been calibrated by comparison with absolute ages derived from tree rings. This calibration has now been extended back about 12,000 years. Thus, accurate ages ^{14}C ages can be obtained despite production rate variations. Currently, an effort is under way to calibrate ^{14}C ages back 50,000 years by comparing then with ^{230Th}/^{238}U ages of corals. The discrepancy between ^{14}C ages and other chronometers such as tree rings and ^{230Th}/^{238}U ages provides a measure of the ^{14}C production rate and cosmic ray flux. That provides an indirect measure past solar activity. Solar activity in turn has a direct effect on terrestrial climate, and hence must be constrained if past climatic variations are to be understood.

Other interesting applications include determining the 'age' of deep water in the oceans, which we will discuss in Chapter 15. By comparing ^{14}C/^{12}C ratios of benthic and planktonic foraminifera in a single sedimentary horizon, it is possible to determine bottom water ages in the past, and hence constrain 'paleocirculation' rates.

Other cosmogenic isotopes have been used to determine sedimentation rates, growth rate of Mn nodules where ages are too old for U-series disequilibrium techniques, and the ages of ice in Greenland and Antarctic ice cores.

8.5.2 ^{36}Cl in Hydrology

^{36}Cl has been applied to hydrological problems for some time. The general principle is that ^{36}Cl is produced at a constant rate in the atmosphere, carried to the surface of the Earth in rain and incorporated into hydrological systems. Cl is an excellent candidate element for such studies because it should remain in solution in most instances, and hence the only loss should be through radioactive decay. Imagine a simple system in which rainwater is incorporated into an aquifer at some unknown time in the past. In this case, if we can specify the number of ^{36}Cl atoms per liter in rain (and if we can assume this value is time-invariant), then we can determine the age of water in the aquifer by measuring the number of ^{36}Cl atoms per liter since:

$$^{36}\text{Cl} = {}^{36}\text{Cl}° \, e^{-\lambda t}$$

8.57

Determining the age of water in underground aquifers is an important problem because of the increasing demands placed in many parts of the world on limited water resources. A prudent policy for water resource management is to withdraw from a reservoir at a rate no greater than the recharge rate. Determination of recharge rate is thus prerequisite to wise management.

Dealing with just the number, or concentration, of ^{36}Cl atoms can have disadvantages, and can be misleading. Evaporation, for example, would increase the number of ^{36}Cl atoms. Thus the $^{36}Cl/Cl$ ratio (Cl has two stable isotopes: ^{35}Cl and ^{37}Cl) is often used. This also can have problems since chlorine can be leached from rocks. This chlorine will be nearly free of ^{36}Cl (some ^{36}Cl will be produced naturally by neutron capture), and hence this process will decrease the $^{36}Cl/Cl$ ratio. Further complications arise from the nuclear bomb-produced ^{36}Cl. Particularly large amounts were produced by nuclear bomb testing at sea, where bomb-produced neutrons were captured by ^{35}Cl in seawater.

Table 8.6. ^{36}Cl MEASUREMENTS IN THE DEAD SEA SYSTEM

Site	$^{36}Cl/Cl$ (10^{-15}) mg/l	Cl 10^6 atoms/l	^{36}Cl
Mt. Hermon Snow	1580±120	1.50	40±5
Banias River	400±60	11.9	80±15
Snir River	430±125	11.0	80±20
Dan River	725±140	10.5	129±25
Lake Kinneret	49±15	252	210±65
Jordan River	121±19	646	1,320±210
Dead Sea	17±2	2.30×10^5	6.6×10^4
Ashlag Spring (saline spring)	4±2	2.6×10^5	

In a somewhat different application, Paul et al. (1986) used ^{36}Cl to determine the accumulation time of dissolved salt in the Dead Sea. The Dead Sea is a particularly simply hydrologic system because it has no outlet. In such a simple system, we can describe the variation of the number of ^{36}Cl atoms with time as the rate of input less the rate of decay:

$$\frac{dN}{dt} = I - \lambda t \qquad \qquad 8.58$$

where I is the input rate (precipitation of chloride is assumed negligible). Integration of this equation yields:

$$N = \frac{I}{\lambda}(1 - e^{-\lambda t}) \qquad \qquad 8.59$$

Paul et al. measured $^{36}Cl/Cl$ in Mt. Hermon snow, in various rivers in the Dead Sea system, and in saline springs in the Dead Sea basin. These results are summarized in Table 8.6. Using equation 8.58, they estimated an accumulation time of 20,000 years for the salt in the Dead Sea. The Dead Sea basin has been estimated to be 15,000 years old based on ^{14}C. The difference suggests some of the Cl now in the Dead Sea was inherited from its less saline Pleistocene predecessor, Lake Lisan. The data in Table also illustrates how a combination of Cl and ^{36}Cl data can distinguish between addition of Cl from rock leaching and evaporation, both of which are processes that will increase the concentration of Cl. Evaporation should not significantly change the $^{36}Cl/Cl$ ratio, while addition of Cl derived from rock leaching should decrease this ratio. There is a general southward (downstream) increase in Cl concentration in the Jordan River—Dead Sea system. It is apparent from the data in Table 8.6 that this is due to both addition of rock-derived Cl and evaporation.

8.5.3 ^{10}Be in Subduction Zone Studies

One of the usual uses of cosmogenic nuclides is the use of ^{10}Be to trace sediment subduction (Tera et al., 1986). Since ^{10}Be does not exist in the Earth's interior, its presence there could result only from subduction of sediment (which concentrates cosmogenic ^{10}Be). ^{10}Be has been identified in some island arc volcanics, but not in other volcanic rocks (at least not above the background level of 10^6 atoms per gram, i.e. 1 atom in 10^{18}). This is strong evidence that subducted sediment plays a role in island arc magma genesis, something suspected on the basis of other geochemical evidence. We'll examine this application of cosmogenic isotopes in more detail in Chapter 12.

8.5.3 Cosmic-Ray Exposure Ages of Meteorites

The surfaces of meteorites in space are subject to a fairly high cosmic ray flux because there is no atmosphere to protect them. This leads to another interesting application of cosmogenic isotopes: 'cosmic ray exposure ages'. Here rare stable isotopes are used rather than radioactive ones because of the long times involved. For example, potassium is not present naturally in iron meteorites, but is produced by cosmic ray interactions. Knowing the production rate of ^{41}K and its abundance, it is possible to calculate how long a meteorite has been exposed to cosmic rays. Two important results of such studies are worth mentioning: (1) exposure ages are much younger than formation ages and (2) meteorites that are compositionally and petrologically similar tend to have similar exposure ages (Figure 8.26). This means meteorites now colliding with the Earth have not existed as small bodies since the solar system formed. Instead, they are probably more or less continually (on a time scale of 10^9 yr) produced by breakup of larger bodies through collisions. Also, similar meteorites probably come from the same parent body.

8.5.3 Fossil Nuclides

Finally, there is evidence short-lived isotopes existed in abundance when the solar system formed. They must have been created shortly before, implying a nucleosynthetic process, such as a red giant star or a supernova event shortly before the formation of the Earth. Some of these isotopes (e.g., ^{26}Al) may have been sufficiently abundant that they could have been significant heat sources early in the history of the Earth and other planetary bodies. Evidence of their existence comes from non-uniform distribution of their daughter products. For example, if ^{26}Mg, the daughter of ^{26}Al, were found be more abundant in an Al-rich phase such as plagioclase or
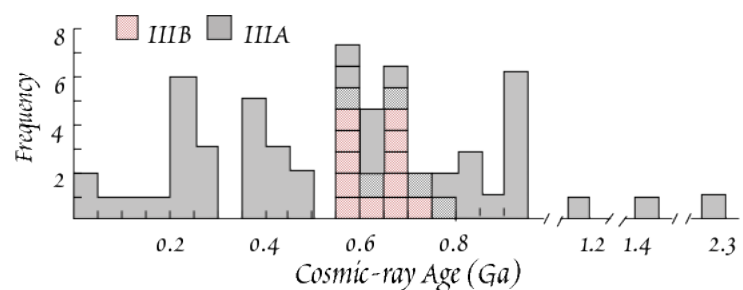

Figure 8.26. Cosmic-Ray exposure age distribution in iron meteorites. Seventeen of 18 IIIAB irons fall in a cluster at 650±100 Ma (after Voshage, 1967).

spinel than in olivine, one might conclude the excess ^{26}Mg was produced by the decay of ^{26}Al. There is only one example of non-homogeneous distribution of the daughter of a fossil radionuclide in the Earth: ^{129}Xe, the daughter of ^{129}I. Excess ^{129}Xe has been identified in CO_2 well gas and in some oceanic basalts. The implication is first, the Earth formed before ^{129}I decayed away, and second, there was probably a major outgassing event very early in which most of the Xe went into the atmosphere. ^{129}I remained in the solid Earth, decaying to ^{129}Xe. As a result, the Xe that remained in the Earth was richer in ^{129}Xe.

References and Suggestions for Further Reading:

Allégre, C. J., and J. M. Luck. 1980. Osmium isotopes as petrogenic and geologic tracers, *Earth Planet. Sci. Lett.*, 48: 148-154.

Allegre, C. J., A. W. Hofmann and K. O'Nions, 1996. The argon constraints on mantle structure, *Geophysical Research Letters*, 23: 3555-3557.

Allègre, C. J., P. Sarda and T. Staudacher. 1993. Speculations about the cosmic origin of He and Ne in the interior of the Earth, *Earth Planet. Sci. Lett.*, 117, 229-233, 1993.

Clark, W. B, M. A. Beg, and H. Craig. 1969. Excess ^{3}He in the sea: evidence for terrestrial primordial helium, *Earth Planet. Sci. Lett.*, 6: 213-230, 1969.

Creaser, R. A., D. A. Papanastassiou and G. J. Wasserburg. 1991. Negative thermal ion mass spectrometry of osmium, rhenium, and iridium. *Geochim. Cosmochim. Acta*. 55: 397-401.

DePaolo, D. J. 1988. *Neodymium Isotope Geochemistry, an Introduction*, Berlin: Springer-Verlag.

DePaolo, D. J. 1981. Neodymium isotopes in the Colorado Front Range and crust mantle evolution in the Proterozoic, *Nature*, 291, 193-196.

Dickin, A. P., Cerium isotope geochemistry of ocean island basalts, *Nature*, 326: 283-284, 1987.

Dickin, A. 1995. *Radiogenic Isotope Geochemistry*. Cambridge: Cambridge University Press.

Esser, B. K. and K. K. Turekian. 1993. The osmium isotopic composition of the continental crust. *Geochimica et Cosmochimica Acta.* 57: 3093-3104.

Farley, K. A. and R. J. Poreda. 1993., Mantle neon and atmospheric contamination, *Earth Planet. Sci. Lett.*, 114, 325-339.

Faure, G. 1986. *Principles of Isotope Geology*, 2nd ed., New York: Wiley & Sons.

Gast, P. W. 1960. Limitations on the composition of the upper mantle, *J. Geophys. Res.*, 65: 1287-1297.

Hauri, E. H. and S. R. Hart. 1993. Re-Os isotope systematics of HIMU and EMII oceanic island basalts from the south Pacific Ocean. *Earth Planet. Sci. Lett.* 114: 353-371.

Hirt, B., W. Herr and W. Hoffmester. 1963. Age determinations by the rhenium-osmium method. in *Radioactive Dating,* ed. 35-44. Vienna: Internation. Atom Energy Agency.

Honda, M., M. I., D. Patterson, A. Doulgeris and D. Clague, Possible solar noble-gas component in Hawaiian basalts, *Nature*, 349, 149-151, 1991.

Huh, C.-A. and T.-L. Ku. 1984. Radiochemical observations on manganese nodules from three sedimentary environments in the north Pacific, *Geochim. Cosmochim. Acta*, 48. 951-964.

Kurz, M. D. 1987. In situ production of terrestrial cosmogenic helium and some applications to gechronology, *Geochim. et Cosmochim. Acta*, 50: 2855–2862.

Kurz, M. D., W. J. Jenkins, and S. R. Hart. 1982. Helium isotopic systematics of oceanic islands and mantle heterogeneity, *Nature*, 297: 43-47.

Luck, J.-M., J.-L. Birck and C. J. Allegre. 1980. ^{187}Re-^{187}Os systematics in meteorites: Early chronology of the solar system and age of the Galaxy. *Nature*. 283: 256-259.

Lupton J. E. and H. Craig. 1981. A major ^{3}He source on the East Pacific Rise, *Science,* 214: 13-18.

Lupton, J. E. 1983. Terrestrial inert gases: isotopic tracer studies and clues to primordial components in the mantle, *Ann. Rev. Earth. Planet. Sci.,* 11: 371-414.

Lupton, J. G. and H. Craig. 1975 Excess ^{3}He in oceanic basalts: evidence for terrestrial primordial helium, *Earth. Planet. Sci. Lett.,* 26: 133-.

Marshall, B. D. and D. J. DePaolo, Initial Ca isotope variations in igneous rocks: implications for petrogenetic models and the composition of the lower crust, *EOS*, 68; 465, 1987.

Martin, C. E. 1991. Osmium isotopic characteristics of mantle-derived rocks, *Geochim. Cosmochim. Acta*, 55, 1421-1434.

Nyquist, L. E., D. D. Bogard, H. Wiesmann, B. M. Bansal., C.-Y. Shih and R. M. Morris. 1990. Age of a eucrite clase from the Bholghati howardite. *Geochim. Cosmochim. Acta*. 54: 2195-2206.

Ozima, M. and K. Zahnle. 1993. Mantle degassing and atmospheric evolution: noble gas view, *Geochem. J.*, 27, 185-200.

Patchett, P. J. 1983. Importance of the Lu-Hf isotopic system in studies of planetary chronology and chemical evolution, *Geochim. Cosmochim. Acta*, 47: 81-91.

Patchett, P. J., W. M. White, H. Feldmann, S. Kielinczuk and A. W. Hofmann. 1984. Hafnium/rare earth element fractionation in the sedimentary system and crustal recycling into the Earth's mantle. *Earth. Planet. Sci. Lett.* 69: 365-378.

Paul, M., A. Kaufman, M. Magaritz, D. Fink, W. Henning, et al. 1986. A new ^{36}Cl hydrological model and ^{36}Cl systematics in the Jordan River/Dead Sea system, *Nature*, 29, 511-515.

Peucker-Ehrenbrink, B., G. Ravissa and A. W. Hoffmann. 1995. The marine ^{187}Os/^{186}Os record of the past 80 million years. *Earth Planet. Sci. Lett.* 130: 155-167.

Poreda, R. J. and K. A. Farley, Rare gases in Samoan xenoliths. 1992. *Earth Planet. Sci. Lett.*, 113, 129-144.

Reisberg, L., A. Zindler, F. Marcantonio, W. M. White, D. Wyman, and B. Weaver. 1993. Os isotope systematics in ocean island basalts. *Earth Planet. Sci. Lett.* 120: 149-167.

Sarda, P., T. Staudacher and C. J. Allègre. 1988. Neon isotopes in submarine basalts, *Earth Planet. Sci. Lett.*, 91, 73-88.

Tera, F., L. Brown, J. Morris, I. S. Sacks, J. Klein, R. Klein and R. Middleton. 1986. sediment incorporation in island-arc magmas: inferences from ^{10}Be, *Geochim. Cosmochim. Acta*, 50: 535-550.

Volpe, A. M. and P. E. Hammond. 1991. ^{238}U-^{230}Th-^{226}Ra disequilibria in young Mount St. Helens rocks: time constraint for magma formation and crystallization, *Earth Planet. Sci. Lett.*, 107, 475-486.

Voshage, H. 1967. Bestrahlungsalter und Herkunft der Eisenmeteorite, *Z. Naturforschung,* 22a: 477-506.

Walker, R. J., R. W. Carlson, S. B. Shirey and F. R. Boyd. 1989. Os, Sr, Nd, and Pb isotope systematics of southern African peridotite xenoliths: implications for the chemical evolution of the subcontinental mantle. *Geochim. Cosmochim. Acta*. 53: 1583-1595.

White, W. M., P. J. Patchett and D. BenOthman. 1986. Hf isotope ratios of marine sediments and Mn nodules: evidence for a mantle source of Hf in seawater. *Earth Planet. Sci. Lett.* 79: 46-54.

York, D. 1969. Least squares fitting of a straight line with correlated errors, *Earth Planet. Sci. Lett.*, 5, 320-324.

Zindler, A. and S. R. Hart. 1986. Helium: problematic primordial signals, *Earth. Planet Sci. Lett.*, 79: 1-8.

PROBLEMS

1. A few years ago, chemists at the University of Utah claimed to have succeeded with a 'cold' fusion experiment in which deuterium nuclei fuse to produce a ^{3}He nucleus and a neutron, i.e.:

$$^2H + {}^2H \rightarrow {}^3He + n$$
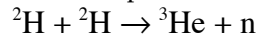
If the mass of ^{2}H is 2.0141077 u, the mass of ^{3}He is 3.01602929 u, the mass of a neutron is 1.00866489 u, and normal water has $^2H/^1H = 1.4 \times 10^{-4}$, what is the energy yield (in kJ) of this reaction per mole of normal water? (Don't forget that each reaction requires two deuterons).

2. What are the binding energies per nucleon of ^{147}Sm (mass = 146.914907 u) and ^{143}Nd (mass = 142.909823)?

3. Calculate the maximum β^- energy in the decay of ^{87}Rb to ^{87}Sr. The mass of ^{87}Rb is 86.9091836 u; the mass of ^{87}Sr is 86.9088902 u.

4. What is the decay constant (λ) of ^{152}Gd if its half-life is 1.1×10^{14} yr?

5. The following data were measured on whole rock gneiss samples from the Bighorn Mountains of Wyoming. Use linear regression to calculate the age and initial $^{87}Sr/^{86}Sr$ for this gneiss.

Sample	$^{87}Rb/^{86}Sr$	$^{87}Sr/^{86}Sr$
4173	0.1475	0.7073
3400	0.2231	0.7106
7112	0.8096	0.7344
3432	1.1084	0.7456
3422	1.4995	0.7607
83	1.8825	0.7793

6. The following were measured on a komatiite flow in Canada. Use simple linear regression to calculate slope. Plot the data on isochron diagrams.

	$^{147}Sm/^{144}Nd$	$^{143}Nd/^{144}Nd$
M654	0.2427	0.513586
M656	0.2402	0.513548
M663	0.2567	0.513853
M657	0.2381	0.513511
AX14	0.2250	0.513280
AX25	0.2189	0.513174
M666	0.2563	0.513842
M668	0.2380	0.513522

a. Calculate the Sm-Nd age and the error on the age.

b. Calculate the initial ε_{Nd} (i.e., the ε_{Nd} at the age you calculate in a.) and the error on the initial ε_{Nd}.

7. A sample of granite has $^{143}Nd/^{144}Nd$ and $^{147}Sm/^{144}Nd$ of 0.51215 and 0.1342, respectively. The present chondritic $^{143}Nd/^{144}Nd$ and $^{147}Sm/^{144}Nd$ are 0.512638 and 0.1967, respectively. The decay constant of ^{147}Sm is 6.54×10^{-12} Ga^{-1}. Calculate the τ_{CHUR}, i.e., crustal residence time relative to a chondritic mantle, for this granite.

8. Imagine that an initially uniform silicate Earth underwent melting at some time in the past to form continental crust (melt) and mantle (melting residue). Calculate the present day Sr and Nd isotopic composition of 1%, 2%, and 5% partial melts and respective melting residues assuming the bulk partition coefficients given in Example 8.4. Assume that the present day $^{87}Rb/^{86}Sr$, $^{87}Sr/^{86}Sr$, $^{147}Sm/^{144}Nd$, $^{143}Nd/^{144}Nd$ ratios of the bulk silicate Earth are 0.085, 0.705, and 0.1967, and 0.512638 respectively. Perform the calculation assuming the melting occurred at 4.0 Gam 3.0 Ga, and 2.0 Ga. Plot your results on a Sr-Nd isotope diagram (i.e., $^{143}Nd/^{144}Nd$ vs. $^{87}Sr/^{86}Sr$).

9. Given the data on a series of whole rocks below, use linear regression to calculate:
(a.) the age of the rocks and the error on the age
(b.) their initial $^{143}Nd/^{144}Nd$, and the error on the initial ratio
(c.) From b, calculate the initial ε_{Nd}, that is, ε_{Nd} at the time calculated in a. Take the present-day chondritic $^{143}Nd/^{144}Nd$ to be 0.512638 and the (present-day) chondritic $^{147}Sm/^{144}Nd$ to be 0.1967 (you need to calculate the chondritic value at the time the rock formed to calculate initial ε_{Nd}).
(d.) Calculate the depleted mantle model age τ_{DM}. Assume that the present $^{143}Nd/^{144}Nd$ of the depleted mantle is 0.51310, and that the depleted mantle has evolved from the chondritic initial with a constant $^{147}Sm/^{144}Nd$ since 4.55 Ga. How does it compare to the age you calculated in (a.)?

sample	$^{147}Sm/^{144}Nd$	$^{143}Nd/^{144}Nd$
whole rock	0.1886	0.512360
garnet	0.6419	0.513401
clinopyroxene	0.1146	0.512245

Linear regression functions are available on some scientific calculators and in statistical packages for microcomputers, and in Microsoft Excel. Alternatively, use the equations in Appendix 3.

10. The following were measured on a komatiite flow in Canada. Use simple linear regresssion to calculate slopes. Plot the data on isochron diagrams.

	$^{206}Pb/^{204}Pb$	$^{207}Pb/^{204}Pb$	$^{208}Pb/^{204}Pb$
M665	15.718	14.920	35.504
M654	15.970	14.976	35.920
M656	22.563	16.213	41.225
M663	16.329	15.132	35.569
M657	29.995	17.565	48.690
AX14	32.477	17.730	49.996
AX25	15.869	14.963	35.465
M667	14.219	17.717	33.786
M666	16.770	15.110	35.848
M668	16.351	15.047	36.060
M658	20.122	15.700	39.390

a. Calculate the Pb-Pb age and the error on the age.
b. Calculate the Th/U ratio of the samples.

11. Calculate the $^{207}Pb/^{204}Pb$—$^{206}Pb/^{204}Pb$ age for the rocks below. (Hint, first calculate the slope using linear regression, then use Excel's Solver to calculate the age).

sample	$^{206}Pb/^{204}Pb$	$^{207}Pb/^{204}Pb$
NPA5	15.968	14.823
NPA12	17.110	15.043
NPA15	17.334	15.090
NPA15HF	17.455	15.104

12. a.) Calculate the isotopic evolution ($^{207}Pb/^{204}Pb$ and $^{206}Pb/^{204}Pb$ only) of Pb in a reservoir having a $^{238}U/^{204}Pb$ of 8. Do the calculation at 0.5 Ga intervals from 4.5 Ga to present. Assume the reservoir started with Canyon Diablo initial Pb isotopic composition. Plot your results on a $^{207}Pb/^{204}Pb$ vs $^{206}Pb/^{204}Pb$ graph.

b.) Calculate the isotopic evolution ($^{207}Pb/^{204}Pb$ and $^{206}Pb/^{204}Pb$ only) of Pb in a reservoir having a $^{238}U/^{204}Pb$ of 7 from 4.5 to 2.5 Ga and $^{238}U/^{204}Pb$ of 9 from 2.5 Ga to present. Do the calculation at 0.5 Ga intervals from 4.5 Ga to present. Assume the reservoir started with Canyon Diablo initial Pb isotopic composition. Plot your results on a $^{207}Pb/^{204}Pb$ vs $^{206}Pb/^{204}Pb$ graph.

HINT: the equation: $\qquad ^{206}Pb/\,^{204}Pb = \,^{206}Pb/\,^{204}Pb_0 + \mu(e^{\lambda_{238}t} - 1)$

is valid for calculating the growth of $^{206}Pb/^{204}Pb$ only between the present and the initial time; i.e., the time when $^{206}Pb/^{204}Pb = (^{206}Pb/^{204}Pb)_o$ (because the $^{238}U/^{204}Pb$ ratio used is the present ratio). The growth of $^{206}Pb/^{204}Pb$ between two other times, t_1 and t_2, where t_1 is older than t_2, may be calculated by calculating the growth of $^{206}Pb/^{204}Pb$ between t_2 and the present, and between t_1 and the present and subtracting the latter from the former. If μ_1 is the value of μ between t_1 and t_2, and μ_2 is the value of μ between t_2 and the present, the relevant equation is then:

$$^{206}Pb/\,^{204}Pb = (^{206}Pb/\,^{204}Pb)_{t_1} + \mu_1(e^{\lambda_{238}t_1} - 1) + \mu_2(e^{\lambda_{238}t_2} - 1)$$

if $\mu_1 = \mu_2$ then the equation simplifies to:

$$^{206}Pb/\,^{204}Pb = (^{206}Pb/\,^{204}Pb)_{t_1} + \mu(e^{\lambda_{238}t_1} - e^{\lambda_{238}t_2})$$

13. A basalt from Réunion has a $(^{230}Th/^{232}Th)$ ratio of 0.93 and a $(^{238}U/^{232}Th)$ ratio of 0.75. Assuming the age of the basalt is 0:
   a.) what is the $(^{238}U/^{232}Th)$ ratio of the source of the basalt?
   b.) what is the $^{232}Th/^{238}U$ *atomic* ratio of the source of the basalt?
   c.) assuming bulk distribution coefficients of 0.01 for U and 0.005 for Th and equilibrium melting, what is the percent melting involved in generating this basalt?
(remember the parentheses denote *activity* ratios).

14. Given the following data on the Cheire de Mazaye Flow in the Massif Central, France, calculate the age of the flow and the initial $^{232}Th/^{238}U$ (atomic). Use simple linear regression in obtaining your solution.

	$(^{238}U/^{232}Th)$	$(^{230}Th/^{232}Th)$
whole rock	0.744	0.780±0.012
magnetite M1 (80-23μ)	0.970	0.864±0.017
magnetite M2 (23-7μ)	1.142	0.904±0.017
clinopyroxene	0.750	0.791±0.019
plagioclase	0.685	0.783±0.018